Aus dem Institut für Biosynthese neuraler Strukturen

des Zentrums für Molekulare Neurobiologie Hamburg

des Universitätsklinikums Hamburg-Eppendorf

Direktorin: Frau Prof. Dr. Melitta Schachner

Age dependent and region-specific alterations in the brain of CHL1

deficient mice: an emerging animal-based model of schizophrenia

Dissertation

zur Erlangung des Grades eines Doktors der Medizin

dem Fachbereich Medizin der Universität Hamburg vorgelegt von

Barbara Elisabeth Thilo

aus Bonn

Hamburg 2005

Angenommen vom Fachbereich Medizin

der Universität Hamburg am: 12.12.2005

Veröffentlicht mit Genehmigung des Fachbereichs

Medizin der Universität Hamburg

Prüfungsausschuss, der/die Vorsitzende: Prof. Dr. M. Schachner

Prüfungsausschuss: 2. Gutachter/in: PD Dr. A. Irintchev

Prüfungsausschuss: 3. Gutachter/in: Prof. Dr. M. Davidoff

CONTENTS

CONTENTS

CONTENTS

1 INTRODUCTION

1.1 Cell Adhesion Molecules

Cell migration, cell adhesion, neurite outgrowth, axon fasciculation and synapse stabilization are crucial events for the construction of the unique brain architecture. They are a requirement for proper cell-cell interaction and synaptic plasticity associated with learning and memory. Disturbances in these processes lead to severe human developmental diseases. A prominent group of molecules mediating those processes are cell adhesion molecules (CAMs).

Cell adhesion molecules are divided into three major families: the integrins, the cadherins and the immunoglobulin superfamily (Figure 1). Those CAMs which are most importantly involved in brain development and function belong to the immunoglobulin (Ig) superfamily which is characterized by the presence of at least one Ig like-domain, enabling them to mediate cell adhesion in a calcium independent manner. The Ig superfamily falls into three subgroups depending on the number of Ig-like domains, the presence and number of fibronectin (FN) III repeats and the mode of attachment to the cell membrane (Cunningham 1995). The neural cell adhesion molecule (NCAM), L1 and the close homologue of L1 (CHL1) are members of subgroup 2 containing Ig-like domains and FN III repeats.

CAMS

Integrins

Cadherins

Immunoglobulin Family

Subgroup 1
only Ig-like domains

Subgroup 2
Ig-like domains + FN domains

Subgroup 3
Ig-like domains + different domains

NCAM

L1
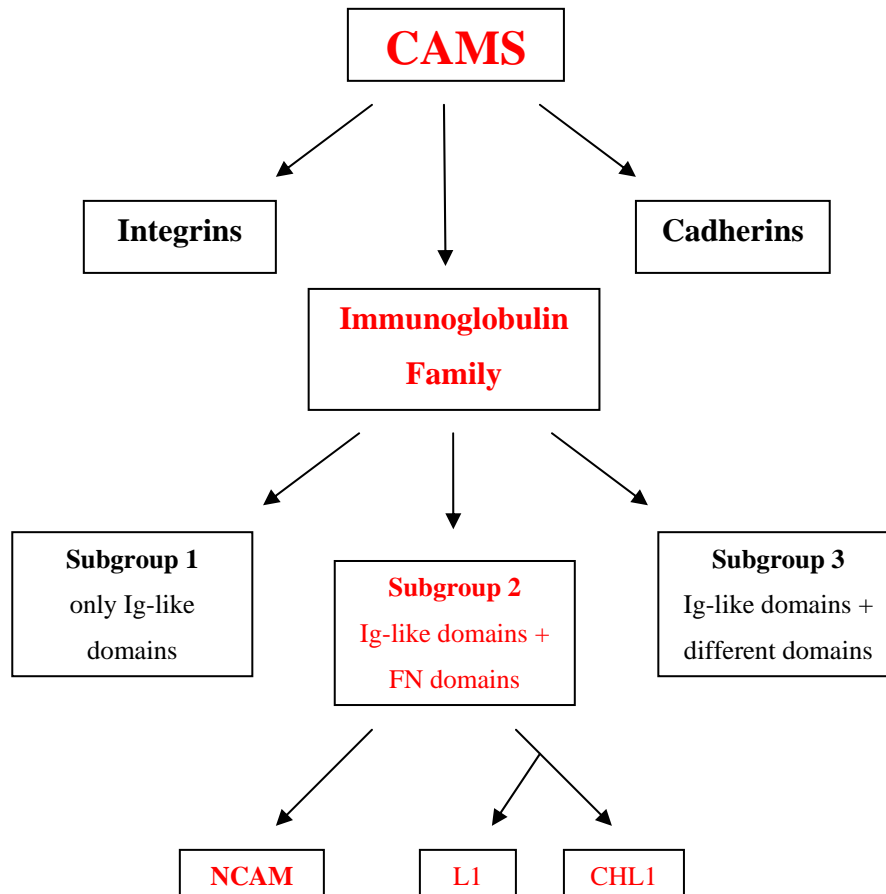
CHL1

Figure 1: The family tree of the cell adhesion molecules (CAMs) CHL1, L1 and NCAM.

1.2 Structure and functional properties of Ig-CAMs

1.2.1 NCAM

NCAM was the first member of the Ig-like cell adhesion molecules to be described (Brackenbury et al. 1977). It consists of five Ig-like domains and two FN type III repeats in the extracellular region (Cunningham et al. 1987). Three major isoforms were found: two isoforms of 140 kD and 180 kD are transmembrane molecules with a short cytoplasmic and a long cytoplasmic domain, respectively. The third form of 120 kD has no cytoplasmic domain and is attached to the cell membrane via a glycophosphatidyl inositol linkage (Owens et al. 1987). All isoforms can mediate homophilic binding, but heterophilic binding has also been described (Cole et al. 1989).

NCAM is the only cell adhesion molecule known to carry a large amount of negatively charged sugar polysialic acid (PSA) influencing the kinetics of NCAM (Hoffman and Edelman 1983) and enhancing axonal growth (Rutishauser and Landmesser 1996).

1.2.2 L1 family

L1 family members have been found in different species, from intervertebrates to mammals. In vertebrates, the L1 family consists of four members: L1, CHL1, neurofascin and NgCAM related cell adhesion molecule (NrCAM). They have a similar structure consisting of six Ig-like domains, four to five FN type III repeats, a transmembrane stretch and a highly conserved cytoplasmic tail. The L1 family members are potent promoters of neurite outgrowth and are expressed relatively late during development. These proteins are prominently expressed by neurons, although some family members are also present on glial cells (Bixby et al. 1988; Collinson et al. 1998; Holm et al. 1996). Several L1 family members can be expressed simultaneously in one set of neuronal cell types, whereas in other subsets of neurons only a particular L1 family member is expressed.

1.2.2.1 L1

L1, the first L1 family member discovered, contains six Ig-like domains, five fibronectin type III-repeats, a transmembrane stretch and a highly conserved cytoplasmic tail. It binds homophilically as well as heterophilically to other Ig cell adhesion molecules (Grumet and Sakurai 1996), integrins (Montgomery et al. 1996) and receptor tyrosine phosphatases (Friedlander et al. 1994). L1 is present in the central and peripheral nervous system (CNS and PNS) but is also expressed in some non-neural tissues. L1 is functionally important in diverse processes like elongation and fasciculation of axons, neuronal survival, migration of neurons and synaptic plasticity (Lagenaur and Lemmon 1987; Fischer et al. 1986; Chen et al. 1999; Lindner et al. 1983; Lüthi et al. 1994).

1.2.2.2 CHL1-the close homologue of L1

CHL1 was discovered when a lambda gtl 1 expression library for cDNA clones was screened with L1 polyclonal antibodies (Tacke et al. 1987) with the aim to find

cDNA clones containing L1. One of the isolated clones contained a partial cDNA sequence with 34% homology to L1. Subsequently a full length cDNA clone was isolated encoding a novel protein of 1209 amino acids with a calculated molecular mass of approximately 135 kD (Holm et al. 1996). This new molecule was named close homologue of L1 (CHL1).

Expression of CHL1 seems to be restricted to the nervous system (Hillenbrand et al. 1999; Holm et al. 1996). The first expression of CHL1 in mice and rats can be detected at embryonic day 13. Until postnatal day 18 CHL1 levels increase and then start declining subsequently to low levels in the mature brain except for areas of high plasticity like the hippocampus where it is expressed throughout adulthood (Hillenbrand et al. 1999). While the expression patterns of L1 and CHL1 overlap considerably there is one striking difference in that CHL1 transcripts can but L1 transcripts can not be found in astrocytes and oligodendrocyte precursor cells (Hillenbrand et al. 1999). Furthermore, CHL1 is expressed by non-myelinating Schwann cells and some neurons in the PNS (Hillenbrand et al. 1999).

CHL1 consists of the same structural elements as the other members of the L1 family, it shares 60% amino acid identity with L1 in the extracellular region and 40% identity in the cytoplasmic domain. The functional properties have not been as intensively investigated as those of L1. In vitro studies have shown that CHL1 is able to promote neurite elongation and neurite survival (Chen et al. 1999). Recent findings suggest an important role of CHL1 in lesioned nervous tissue since CHL1 is strikingly upregulated in Schwann cells and sensory neurons after nerve crush injury (Zhang et al. 2000). Adult neurons of the central nervous system are also able to up-regulate CHL1 expression after a lesion provided their axons can regrow in a permissive environment like that of a peripheral nerve graft (Chaisuksunt et al. 2000a; Chaisuksunt et al. 2000b).

1.3 CAM knockout mice-their connection to human diseases

1.3.1 NCAM

Several hallmarks of schizophrenia have been encountered in NCAM deficient mice: increased size of lateral brain ventricles (Wood et al. 1998), defects in the structure of the hippocampus (Tomasiewicz et al. 1993), impaired sensory motor gating manifested by reduced prepulse inhibition (PPI) of acoustic startle response (Wood et

al. 1998) and deficits in hippocampus/amygdala dependent learning and Long Term Potentiation (LTP) (Cremer et al. 1994). In particular the hippocampal mossy fibers produce ectopic synapses due to a failure in remodeling (Seki and Rutishauser 1998). Furthermore, NCAM-/- mice are more aggressive and anxious than wild types (Storck et al. 1997).

When brains of schizophrenic patients were analyzed regarding NCAM not only a reduction in polysialylated NCAM in the hippocampus (required for proper axon guidance) was observed (Barbeau et al. 1995) but also an increased NCAM concentration in the cerebrospinal fluid (CSF) was found in patients with schizophrenia compared to healthy individuals (Poltorak et al. 1995).

1.3.2 L1

L1 deficient mice have been generated in two laboratories by homologous recombination (Cohen et al. 1997; Dahme et al. 1997). Both lines have a similar phenotype: abnormally large ventricles, an underdeveloped corticospinal tract (CST), malformations of subsets of cortical dendrites, a reduced size of the corpus callosum, an abnormal association of axons with nonmyelinating Schwann cells, poor spatial learning (Fransen et al. 1998) and a reduced sensitivity to touch and pain. Not only does L1 contribute to LTP (Luthl et al. 1994) but the perturbation of L1 by specific antibodies also leads to alteration in learning and memory (Scholey et al. 1995).

Mutations in the human L1 gene, which is located on the X chromosome, cause a syndrome currently known as L1 disease (Weller and Gärtner 2001). Clinical manifestations range from mild symptoms to severe dysfunctions such as corpus callosum hypoplasia, retardation, adducted thumbs, spastic paraplegia and hydrocephalus (Fransen et al. 1995). The estimated incidence of this syndrome ranges from one in 25000 to one in 60000 male births.

1.3.3 CHL1

In order to gain further insight into the function of CHL1, a CHL1 null mutant mouse was generated by disruption of the ribosomal binding site, the translation initiation codon and the amino terminus including the signal sequence (Montag-Sallaz et al. 2002). The gross morphology of most brain regions like thalamus, cerebellum, main fiber tracts and retina in these mice do not differ from wild type mice. Up to now

only a few morphological abnormalities have been detected in CHL1 deficient mice. The hippocampus is likely to be affected especially the mossy fibers which show path finding errors within the CA3 (Cornu Ammon) region, in that a few thin bundles or single mossy fibers project through the pyramidal cell layer of CA3, instead of being organized in clearly seperated supra-and infrapyramidal bundles.

The olfactory bulb also seems to be affected since olfactory neurons in the CHL1 deficient mouse establish contacts with more than one glomerulus, a condition never observed in wild type mice. Additionally, some axons in the mutant abnormally pass through the glomerular layer and form contacts within the external plexiform layer (Montag-Sallaz et al. 2002).

A striking finding in the CHL1 mutant mouse is a significant up-regulation of NCAM 180 in the olfactory bulb, the cortex, the hippocampus and the amygdala which are brain regions with high levels of CHL1 expression in the adult wild type mouse characterized by a high degree of synaptic plasticity throughout life (Montag-Sallaz et al. 2002). These findings demonstrate similar and perhaps overlapping functions of both molecules *in vivo*. Thus, the enhanced expression of NCAM in the CHL1 mutant mouse might be indicative for compensatory functions of NCAM in the CHL1 deficient mouse.

CHL1 deficient mice do not differ from control wild type animals with respect to general behavior, neurological reflexes, and sensory functions (Montag-Sallaz et al. 2002). They are viable and fertile and have a normal life span. Significant differences between mutants and wild type animals have been observed in the open field paradigm. The mutants spend more time in the central area, which may indicate a reduction of anxiety or a different exploratory behavior. The observation that CHL1 deficient mice have shown significant differences in the Morris water maze as compared to littermates with respect to the path swum parallel to the wall and increased swim path tortuosity, absolute spin, and the time spent in the center quadrant further supports the different exploratory behavior (Montag-Sallaz et al. 2002). Morris water maze is the most popular task in behavioral neuroscience assessing spatial learning and memory in its most basic form.

Considering the fact that CHL1 apparently is a neurodevelopmentally relevant molecule, on one side, and that schizophrenia is a neurodevelopmental disorder, on the other side, a group of Japanese scientists studied the linkage of CHL1 to psychotic diseases (Sakurai et al. 2002). The coding region of the CHL1 gene (Cell adhesion L1

like (CALL) in humans), located on human chromosome 3p26, was screened for mutations in schizophrenic patients. A missense polymorphism (Leu17Phe) was identified which subsequently lead to further examination of the association between the Leu17Phe polymorphism and schizophrenia. It was found that the frequency of leucin at amino acid 17 was significantly higher in patients with schizophrenia. Leu 17 is located in the hydrophobic core region of a signal peptide. Some mutations in the hydrophobic core region of signal sequences have been reported to have a direct correlation with defective protein synthesis and pathological status. The results of this study suggest that the CHL1 protein might be involved in the etiology of schizophrenia. A case-control association study of CHL1 and schizophrenia done in the Chinese population confirms the positive association (Chen et al. 2005).

This conclusion gained further support from a recent genome scan meta-analysis done by a large consortium of geneticists which identified the 3p region to be implicated in schizophrenia (Lewis et al. 2003). Another finding linking the CHL1 gene with pathophysiological mechanisms relevant to schizophrenia is that prepulse inhibition (PPI) of the acoustic startle response in CHL1 mutant animals is disrupted (Irintchev et al. 2004a). PPI of the acoustic startle response is a measure of the ability of the CNS to gate the flow of sensorimotor information. Disturbances in these gating processes are characteristically present in major psychiatric disorders including schizophrenia (Braff et al. 2001; Swerdlow et al. 2001).

The 3p region has also been considered as relevant to cognitive functions and intelligence since mental retardation is a common feature in patients with 3p-and ring chromosome 3-syndromes with breakpoints at 3p25.3 and 3p26.1 (Wilson et al. 1982; Asai et al. 1992). CHL1 maps to chromosome 3p26.1 and is therefore a likely candidate. This possibility has recently been investigated in 14 patients with mental retardation (Frints et al. 2003). CHL1 haploinsufficiency has been found in one of the patients clearly showing the relation of CHL1 to cognition.

1.4 Schizophrenia

1.4.1 Epidemiology

Schizophrenia is one of the most important public health problems that our society is confronted with. Around 1% of the population is affected worldwide. The disease has been known for centuries. It afflicts all ethic backgrounds, socioeconomic

classes and nationalities which indicates, that schizophrenia is not a disease of civilization. Since affected patients very often are not able to manage the life they led before the onset of the disease they require public assistance from governmental social security systems. This makes schizophrenia one of the ten most expensive disorders worldwide. The costs to society are counted in billions of dollars. Schizophrenia is usually first diagnosed between the second and third decades occuring more frequently and severely in men than in women (Black and Andreasen 1999).

1.4.2 Etiology-the "two hit hypothesis"

It is currently believed that schizophrenia is a neurodevelopmental disease resulting from abnormal early brain development and/or impaired postnatal maturation of the brain (Bayer et al. 1999; Lewis and Levitt 2002; McGrath et al. 2003). The complex and varying symptoms of the disease indicate that an interplay of multiple factors rather than one single factor triggers this illness. Both genetic and epigenetic factors have been identified and a hypothesis, the "two hit hypothesis", has been proposed explaining the origins of the disease by at least two subsequent etiological "hits", a genetic predisposition and an epigenetic factor.

1) *Genetic predisposition (first hit)*: The fact that schizophrenia is heritable is well established (Gottesman II 1991). The disease tends to run in families. Its frequency is around tenfold higher in siblings and twin studies have shown a concordance rate of approximately 48% in monozygotic twins and 17% in dizygotic twins (Figure 2). The efforts to identify specific genes related to a susceptibility to the disease have been, however, unsuccessful up to now. Earlier linkage studies have provided evidence for many loci on different chromosomes suggesting that multiple gene loci might be involved (Basset 1991; Cloninger 1997; Karayiorgou and Gogos 1997; Kendler and Diehl 1993; Murphy 1996). More recent studies, in which more powerful methods of genetic analyses have been employed, have also yielded inconclusive results (Harrison and Owen 2003).

2) *Epigenetic factor (second hit)*: A plethora of epidemiological findings has linked schizophrenia to environmental factors (Walker et al. 2004). Among these are obstetric complications (Geddes and Lawrie 1995; McNeil et al. 1996), maternal stress (Myhrman et al. 1996; van Os and Selten 1998), upbringing (Lewis et al. 1992),

maternal dietary insufficiency (Susser et al. 1996), maternal viral infection (Wright et al. 1993) and stress during puberty (Walker et al. 2004).

To put it in a nutshell one could assume that a mutant gene or rather multiple genes form the foundation of the disease acting as a first hit. These genes are involved in key events during neurodevelopment and brain maturation and gene deficiency is either transmitted via the germ-line or arises from a spontaneous somatic mutation early during development. The genesis of schizophrenia, however, also requires an environmental factor. During fetal or postnatal development a second hit leads to a dysfunction considered to be primarily related to synaptic properties (Frankle et al. 2003). The disease does not begin immediately after the "hits" but has a delayed onset, starting sometimes twenty years later. The reasons for this "maturational" delay are completely unknown.
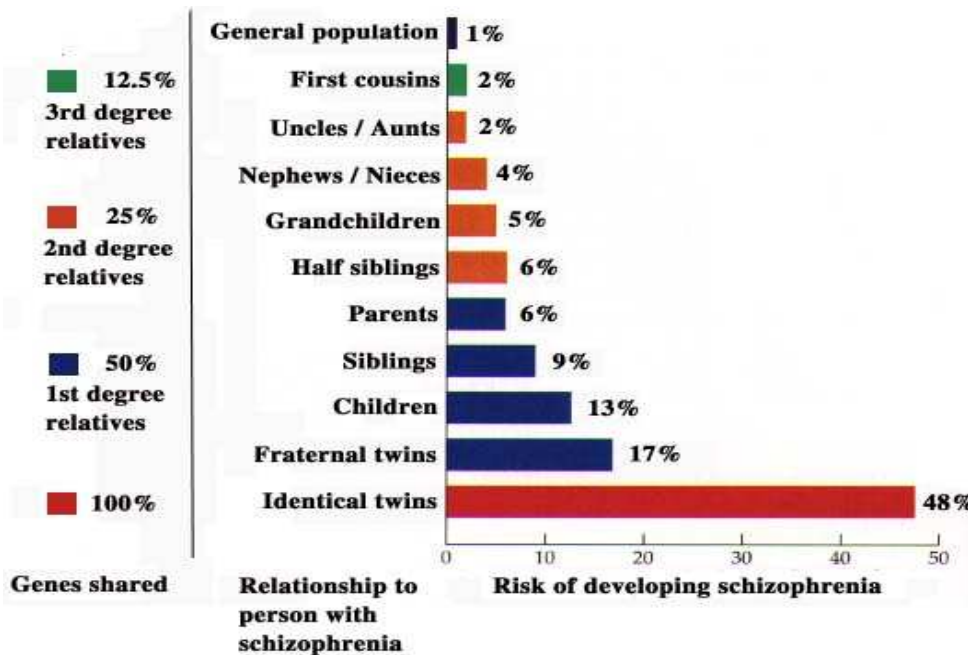
Figure 2: Schizophrenia is hereditary. The graph shows that the disease´s incidence increases with increasing degree of genetic similarity among relatives. From: Gottesman I.I (1991) Schizophrenia Genesis: The Origins of Madness. W.H. Freeman, New York

1.4.3 Clinical manifestation

The course of schizophrenia is characterized by episodes of acute psychotic symptoms followed by phases of remission when symptoms like reduced drive and affect as well as disturbed cognitive functions prevail (Bayer et al. 1999b). The definition of the phenotype in schizophrenia is particularly difficult because patients with this illness suffer from such a diversity of symptoms that the phenotype is defined by criterion-based diagnostic schemes. DSM IV (Diagnostic and Statistical Manual of Mental Disorders) or ICD 10 (International Classification of iseases) take a purely descriptive approach and define schizophrenia on the basis of clinical signs and symptoms.

The symptoms of schizophrenia are classified in four Core Symptom Clusters (Figure 3): **(1) positive symptoms** like halucinations, delusions, disorganized speech and catatonia in which normal functions are distorted and exaggerated; **(2) negative symptoms** like affective flattening, alogia (decrease in the fluency of ideas and language), avolition (decrease in the ability to initiate and pursue goal directed activity) and anhedonia (decrease in the ability to seek out and experience pleasurable activities) which are charaterized by a diminuition or absence of mental functions; **(3) cognitive symptoms** like reduced attention and memory deficits, and **(4) mood symptoms** like depression, suicidality and hopelessness. Together these symptoms lead to social and occupational dysfunction affecting work, interpersonal relationships and self-care (Marder 1999).

(1) Positive symptoms
Delusions
Hallucinations
Disorganized speech

(2) Negative symptoms
Affective flattening
Alogia

**Social/occupational
dysfunction**

(3) Cognitive symptoms
Attention
Memory

(4) Mood symptoms
Dysphoria
Suicidality
Hopelessness
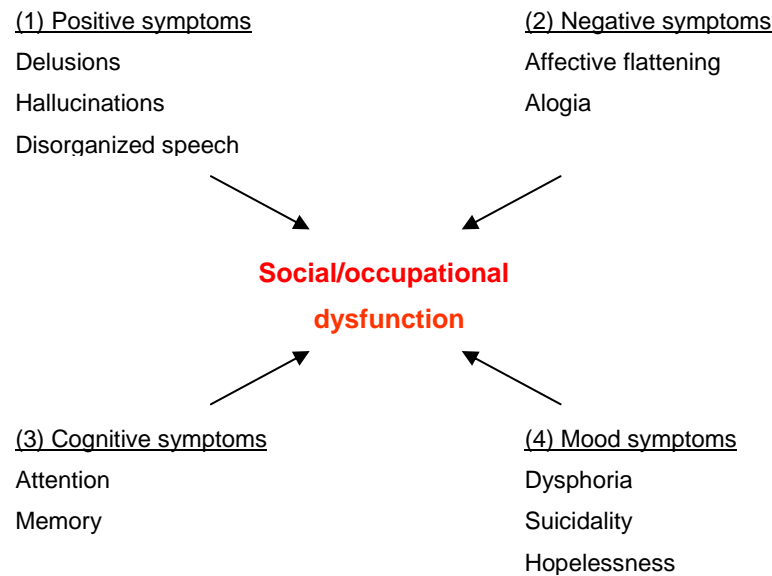
Figure 3: Schizophrenia is characterized by a variety of symptoms categorized in 4 clusters: positive, negative , cognitive and mood symptoms. Combined they lead to social and occupational dysfunction.

1.4.4 Therapy

The current treatment of schizophrenia consists of drug medication and psychotherapy (Walker et al. 2004). The pharmacological treatment, despite the introduction of new drugs over the last years, has a number of insufficiencies among which inefficiency in a substantial proportion of the patients and serious adverse effects are the most troublesome. For antipsychotic medication, neuroleptic drugs are used. The "typical" or "first-generation" neuroleptic drugs, first introduced in the 1950s (chlorpromazine, haloperidol), block dopamine transmission (binding to D_2 receptors) at all sites within the brain where dopamine is used as a transmitter. This includes mesolimbic, mesocortical, nigrostriatal and tuberoinfundibular projections. Blockade in the nigrostriatal pathway results in drug induced EPSS (extrapyramidal signs and symptoms) that partly resemble Parkinson`s disease. The EPSS include increased muscle tone, a fixed facial expression and a stooped, shuffling gait. To counteract the neuroleptic induced EPSS, it became routine to prescribe antiparkinsonian medications in addition (Whitehorn and Kopala 2002). The "atypical" or "second generation" antipsychotic agents (e.g. clozapine) have a more selective effect on dopamine transmission (binding to D_4) and thus produce relatively few EPSS at the usual therapeutic doses. Supportive psychotherapy, used in addition to drug treatment, is not

psychoanalytically orientated but is supposed to give the patient an insight into his disease.

1.4.5 Morphological findings in schizophrenic patients

Although it is generally accepted that schizophrenia is associated with structural brain abnormalities, no aberration has been found that is specific for the disease or present in all patients (Walker et al. 2004). Still, numerous computer tomographies (CT), magnetic resonance imaging (MRI) and postmortem studies have identified brain changes that are consistently observed in many patients (Roberts and Bruton 1990; Knable 1999; Powers 1999; Falkai et al. 2001; McGrath et al. 2003; Walker et al. 2004) such as enlarged ventricles (ventriculomegalia), reduced cortical thickness (frontal and temporal lobes), reduced size of the hippocampus or abnormalities of inhibitory interneurons (e.g. in the prefrontal cortex).

1.5 3p-syndrome

1.5.1 Etiology

The 3p-syndrome results from a deletion of a terminal segment of the short arm of one chromosome 3. Since the clinical manifestation is variable the disorder is thought to be a contiguous gene syndrome with an undefined number of genes contributing to the phenotype. Patients with the most extensive deletions have a more severe phenotype (Drumheller et al. 1996).

1.5.2 Clinical manifestation

The clinical manifestation of the 3p-syndrome is very heterogenous. The syndrome includes low birth weight, growth failure, mental and psychomotor retardation, microcephaly, triangular face, synophrys blepharoptosis, hypertelorism, broad and flat nose, long philtrum, down turned mouth, cleft palate, micrognathia, low-set and malformed ears, finger abnormalities and deafness. Renal anomalies,

gastrointestinal anomalies and congenital heart defects may also be present (Drumheller et al. 1996).

2 RATIONALE AND AIMS OF THE STUDY

Insufficient knowledge with regard to the cause and progression of schizophrenia as well as the heterogeneity of the clinical symptoms have made it difficult to develop a coherent framework suitable for animal modelling (Marcotte et al. 2001). It should be emphasized that it seems impossible to fully reproduce a disorder which affects the highest cognitive functions of a human being in a less cognitively developed animal. Thus, an animal model for schizophrenia is not supposed to serve as the equivalent of the human disorder but should be suitable to test specific causative or mechanistic hypotheses regarding schizophrenia, as well as new medication.

The existing knowledge of the behavior, sensorimotor gating and the brain structure of CHL1 deficient mice provided sufficient evidence to consider it of potential value for neuropsychiatric research. An important step towards further evaluation of the potential of this putative model appeared to be a more detailed analysis of the brain structure in the mutant mouse. The following questions were raised:

- Does the CHL1 deficiency cause developmental gross-anatomical abnormalities such as changes of the total brain mass and volume, brain ventricles, neocortical thickness and size of the hippocampus?

- Are there genotype-related alterations in the size of major neuronal and glial cell populations in areas typically affected in patients with schizophrenia such as the cortex and hippocampus?

- Is there an evidence for abnormalities in nuclei providing dopaminergic innervation of the forebrain?

To answer these questions precisely, a quantitative (stereological) approach appeared most suitable. Such an approach is based on immunohistochemical visualization of defined cell types such as total neuronal population, subpopulations of interneurons, astrocytes, oligodendrocytes and microglia and stereological estimation of cell densities and volumes of structures and has been recently established in the Institute (Irintchev et al. 2004).

A final issue which was addressed while designing this study was the selection of the age at which the animals had to be investigated. Assuming that abnormal postnatal dynamics might be present, and considering the natural history of schizophrenia ("maturational" delayed onset at adolescence or early adulthood, progression in mid-

adulthood), animals at the ages of 2, 6 and 12 months were selected for this investigation.

3 MATERIALS AND METHODS

3.1 Animals

A total of 51 wild-type (CHL1+/+) mice and CHL1-deficient (CHL1-/-) littermates (129Ola-C57BL/6J genetic background, Holm et al. 1996) were used at ages of 2, 6 and 12 months (Table 1). At these ages the animals are in their late adolescence (2 months), early and mid-adulthood (6 and 12 months, respectively). The animals were bred in the SPF (specific pathogen-free) utility of the Univeritätsklinikum Hamburg and delivered to the Institute at the day of sacrifice. All animals used appeared healthy upon arrival and no structural or behavioral abnormalities were noticed. The genotype of the mutant mice had been determined in advance by polymerase chain reaction (PCR) assay as described previously (Kary Mullis 1983). All treatments of the animals were performed in accordance to the German law for protection of experimental animals.

	CHL1+/+ female	CHL1+/+ male	CHL1-/- female	CHL1-/- male
2 months	4	6	6	6
6 months	3	7	6	4
12 months	2	3	0	4

Table 1. Number of animals of different age, genotype and gender used in this study.

## 3.2 Preparation of tissue for sectioning

Mice were weighed and anesthesized with 16% w/v (weight/volume) solution of sodium pentobarbital (Narcoren, Merial, Hallbergmoos, $5\mu l\ g^{-1}$ body weight, i.p.). After surgical tolerance was achieved, the animals were transcardially perfused with physiologic saline for 60 seconds followed by fixative consisting of 4% formaldehyde

and 0.1% $CaCl_2$ in 0.1M cacodylate buffer, pH 7.3 for 15 minutes at room temperature (RT). Cacodylate buffer supplemented with calcium was selected for use in order to ensure optimal tissue fixation including preservation of highly soluble antigens like S100. Following perfusion the brains were left *in situ* for 2 hours at RT to reduce fixation artifacts. Subsequently they were dissected out without the olfactory bulbs and post-fixed overnight (18-22 hours) at 4°C in the formaldehyde solution used for perfusion. Tissue was then immersed into 15% sucrose solution in 0.1M cacodylate buffer, pH 7.3, at 4°C for two days.

Fixed and cryoprotected (sucrose-infiltrated) brains were carefully examined under a stereomicroscope and hair, rests of dura mater or other tissue debri were removed with fine tweezers. Following this, the brains were placed in a mouse brain matrix (World Precision Instruments, Berlin) and the caudal end was cut at a defined level (1 mm from the most caudal slot of the matrix). Then brain mass and volume were measured (see 3.4.1 and 3.4.2). Finally, the brains were frozen by insertion into 2-methyl-butane (isopentane) which had been precooled to -30°C in the cryostat for 2 minutes. The brains were stored in liquid nitrogen until sectioned.

3.3   Preparation of cryostat sections

For sectioning the caudal pole of each brain was attached to a cryostat specimen holder using a drop of distilled water placed on a pre-frozen layer of Tissue Tek (Sakura Finetek Europe, Zoeterwoude, The Netherlands). The ventral surface of the brain was oriented to face the cryostat knife edge and serial coronal sections were cut in a cryostat Leica CM3050 (Leica Instruments, Nußloch, Germany). Sections of 50µm thickness for morphometric analysis were prepared from some brains, the rest were sectioned at 25µm for immunohistochemistry. Sections were collected on SuperFrost Plus glass slides (Roth, Karlsruhe, Germany). Since stereological analyses require extensive sectioning of the structures studied and use of spaced-serial sections (Howard and Reed 1998), sampling was always done in a standard sequence. In the end 4 sections that were 250 or 500µm apart from each other (for 25 and 50µm thick sections, respectively) were present on each slide (Figure 4).
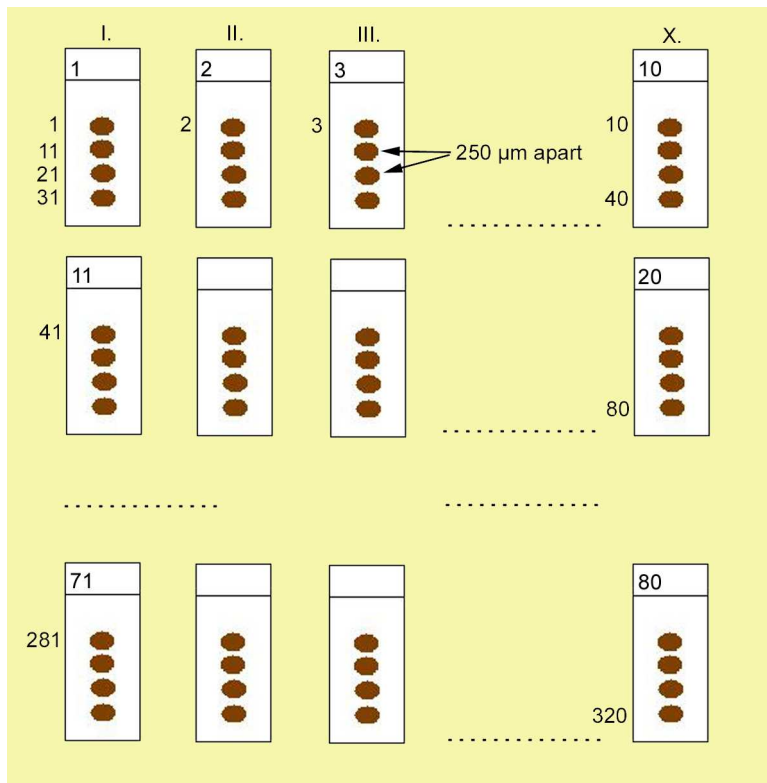
Figure 4: Standardized sequence of collecting sections (25µm) on glass slides. Staining of slides from one row (e.g. 1, 11, etc.) with a given antibody (see below) gives the opportunity to evaluate a cell population using randomly spaced samples from a brain structure of interest.

3.4 Analysis of gross anatomical variables

3.4.1 Brain volume

The brain volume was determined by measurement of volume displacement using a 5 ml measuring cylinder (Roth) prefilled with 4ml sucrose/cacodylate solution.

3.4.2 Brain weight

Brains were blotted with filter paper to remove excess liquid from the surface and the brain mass was measured using a fine 4-digit scale (BP61, Sartorius, Göttingen, Germany).

3.4.3 Ventricles

3.4.3.1 Cresyl Violet-Luxol Fast Blue Staining

Morphometric analysis of the third and the lateral brain ventricles was performed using 50µm or 25µm thick sections stained with cresyl violet and Luxol Fast Blue (Klüver-Barrera procedure optimized for cryostat sections, Geisler et al. 2002). Cresyl violet is a Nissl stain, Luxol Fast Blue delineates myelin (Figure 5). Sections were dehydrated in an ascending series of ethanol (70%, 95% and 100%, 2 minutes each) and stained in 0.1% w/v Luxol Fast Blue (Sigma, Deisenhofen, Germany) solution in 95% ethanol containing 0.05% v/v acetic acid overnight at 37°C. The next day they were washed in 95% ethanol for 3 minutes, then in distilled water. These and all following procedures were performed at room temperature. The differentiation was initiated by immersing the sections in 0.05% w/v aqueous lithium carbonate solution for 3 minutes followed by differentiation in 70% alcohol until gray and white matter were clearly distinguishable (several minutes). The slides were rinsed in distilled water and examined under the microscope. If the differentiation was incomplete, the last step was repeated. After washing the slides in distilled water once again, they were stained in 0.5% w/v cresyl violet acetate (Sigma, Deisenhofen, Germany) solution in 0.1 M acetate buffer, pH 4.0, for 20 minutes followed by washing in distilled water and 70% ethanol (1–2 minutes each). The differentiation was done in cresyl violet differentiator (90ml 95% ethanol, 10ml chloroform, 3 drops glacial acetic acid) for 1-2 seconds. The slides were then immersed in 95% ethanol and absolute ethanol for 2 minutes each and finally cleared in Roticlear (Roth, Karlsruhe, Germany). The differentiation was checked under the microscope to ensure that only nuclei and Nissl substance were stained and the differentiation was repeated, if necessary. Finally the sections were mounted under coverslips with Entellan neu (Merck, Darmstadt, Germany).
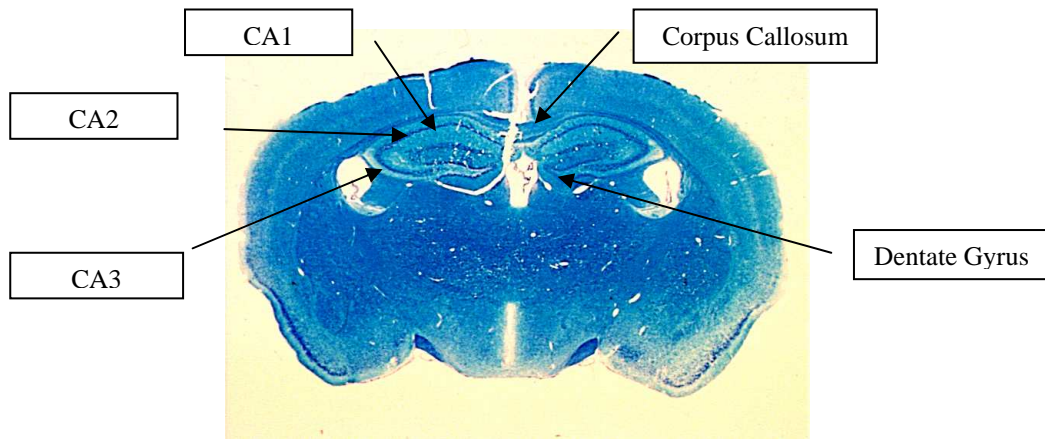
Figure 5: An example of a cresyl violet–Luxol Fast Blue staining of the hippocampus of a 6-month-old CHL1+/+ mouse. Note the clear delineation of major regions such as , e.g. CA1-4 region, Dentate Gyrus, Fibria hippocampi and Corpus Callosum.

3.4.3.2 Cavalieri method

This method of volume estimation is named after the Italian mathematician Bonaventura Cavalieri (1598-1647), a student of Galileo. Being very straightforward to apply it is the most commonly used stereological method for the estimation of a reference volume (Howard and Reed 1998). According to the Cavalieri method, an unbiased estimate of the volume, V, of a structure of interest may be obtained by sectioning it from end to end with a series of systematic sections a constant distance ,T, apart and measuring the area, A, of the transect through the object on each section, whereby:

$$\text{est}_1 V = T(A_1 + A_2 + A_3 + ... + A_m)$$

The volume of the lateral and third ventricles of cresyl violet/Luxol Fast Blue stained spaced-serial sections with T=500µm or T=250µm was measured. The area of each ventricle transect was measured with an Axioskop microscope (Zeiss, objective 10x) equipped with a motorized stage and a Neurolucida software-controlled computer system (MicroBrightField, USA).

3.4.4 Cortical Thickness

To determine the average cortical thickness in the cingulate and motor cortical areas, 25µm sections cut 3 to 4 mm caudally to the rostral pole stained with bis-

benzomide (see 3.5.2) to visualize nuclei were used. The nuclear staining allowed clear distinction of the agranular motor and the granular sensory cortex (M and S and C, respectively, in Figure 6). The area of each cortical field (excluding layer I, see 3.5.3) and the length of its surface boundary were measured directly under the Axioskop microscope using the Neurolucida software (MicroBrightField, USA). The mean cortical thickness was calculated by dividing the area by the length of the superficial boundary.
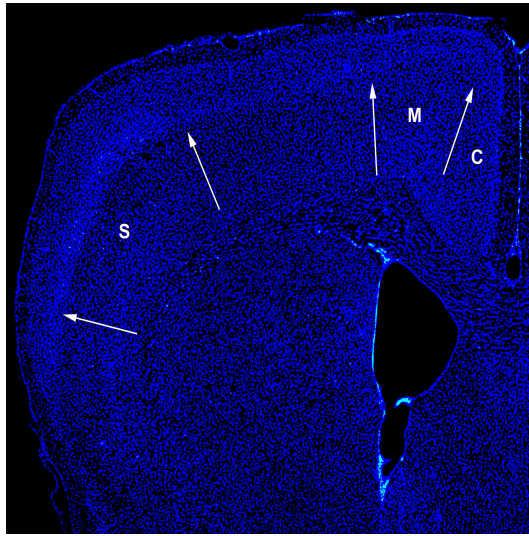
Figure 6: Low magnification view of a coronal brain section from a CHL1+/+ mouse stained with bis-benzimide to visualize nuclei. Nuclear densities and lamination allow precise determination of the boundaries of different cortical areas. S=sensory cortex, M= motor cortex, C= cingulate cortex.

3.4.5 Hippocampus

The areas of the whole hippocampal formation, of the pyramidal cell layer (CA1-3) and of the granular cell layer in the dentate gyrus were measured bilaterally in every animal in three coronal sections with nuclear staining using the Neurolucida system. The criterion for the selection of the mid-section was similarity in appearance to that of section (bregma–2,10 mm) shown in the mouse brain atlas of Sidman et al.. The other two sections were 250µm apart from the mid-section, one rostral to it, one caudal. The average of three values per animals and area was used to calculate group mean values.

3.5 Stereological analysis of immunohistochemically defined cell types

3.5.1 Antibodies

Antibody	Abbreviation	Clone	Producer	Dilution
anti Parvalbumin	anti PV	mouse monoclonal, clone: Parv 19	Sigma, Deisenhofen, Germany	1:1000 9.8µg/ml Ig
anti neuron specific nuclear antigen	anti NeuN	mouse monoclonal, clone: A60	Sigma, Deisenhofen, Germany	1:1000 1µg/ml Ig
anti cyclic nucleotide phosphatase	anti CNP	mouse monoclonal, clone: 11-5B	Sigma Deisenhofen, Germany	1:1000 7.5µg/ml Ig
anti S100	anti S100	rabbit polyclonal, purified IgG fraction	DakoCytomation, Hamburg, Germany	1:500 9µg/ml Ig
anti tyrosine hydroxylase	anti TH	rabbit polyclonal, affinity purified	Chemicon, Hofheim, Germany	1:750 0.1µg/ml Ig
anti reelin	anti reelin	mouse monoclonal, clone: G10	Chemicon, Hofheim, Germany	1:500 2µg/ml Ig
anti Iba-1	anti Iba-1	rabbit polyclonal, affinity purified	Wako Chemicals, Neuss, Germany	1:1500 0.3µg/ml Ig

Table 2: Comercially available antibodies that were used at optimal dilutions for this study. Shown are the abbreviation, the clone, the producer and the dilution that was used.

The antibodies used in this study recognize specific cell-marker antigens known to be expressed in defined cell populations in brain regions that were studied here (Irintchev et al. 2004a):

-NeuN (neuron-specific nuclear antigen) is a protein of unknown function shown to be present in all neurons in the adult brain with the exception of a few cell types which are not found in the cerebral cortex and hippocampus though (Purkinje, mitral and photoreceptor cells, Wolf et al. 1996).

-PV (parvalbumin) is a low molecular weight calcium-binding protein expressed in a major subpopulation of GABAergic neurons in the neocortex and hippocampus.

-Reelin identifies inhibitory interneurons (bitufted, horizontal and Martinotti cells) which do not express PV (Pesold et al. 1999).

-S-100 is a low molecular weight calcium-binding protein expressed in astrocytes.

-CNPase (2´,3´-cyclic nucleotide 3´-phosphodiesterase) is an enzyme only present in cells which are able to synthesize myelin, i.e. oligodendrocytes and Schwann cells.

-Iba1 is a macrophage/microglia-specific calcium-binding protein involved in the activation of quiescent microglial cells (Imai and Kohsaka 2002).

-TH (tyrosine hydroxylase) is the rate-limiting enzyme in the synthesis of the catecholamine neurotransmitters (dopamine, epinephrine, and norepinephrine).

3.5.2 Immunohistochemical stainings

Immunohistochemical stainings were performed as described by Irintchev et al. 2004b. The immunocytochemistry was done on 25µm thick sections. Sections, stored at -20°C, were air-dried for 30 minutes at 37°C. A 10mM sodium citrate solution (pH 9.0, adjusted with 0.1M NaOH) was prepared in a jar and preheated to 80°C in a water bath. The sections were incubated at 80°C for 30 minutes after which the jar was taken out and left to cool down at room temperature. After the slides had cooled down blocking of unspecific binding sites was performed. The sections were incubated at room temperature for one hour in PBS containing 0.2% v/v Triton X-100 (Fluka, Buchs, Germany), 0.02 w/v sodium azide (Merck, Darmstadt, Germany) and 5% v/v normal goat serum (NGS) (Jackson Immuno Research Laboratories, Dianova, Hamburg, Germany). After one hour the blocking solution was aspired and the slides were incubated with the primary antibody diluted in PBS containing 0.5% w/v lamda-

carrageenan and 0.02% w/v sodium azide in PBS. The slides were incubated for 3 days at 4°C in a well closed staining jar. Following this, the sections were washed 3 times in PBS (15 minutes each) before an appropriate (anti-rabbit or anti-mouse) secondary antibody was applied. The sections were incubated with the secondary antibody diluted (1:200) in PBS-carrageenan at RT for 2 hours. Goat anti-rabbit or goat anti mouse IgG conjugated with Cy3 (Jackson Immuno Research Laboratories, Dianova, Hamburg, Germany) was used. After a subsequent wash in PBS, cell nuclei were stained for 10 minutes at room temperature with bis-benzimide solution (Hoechst 33258 dye, 5µg/ml in PBS, Sigma, Deisenhofen, Germany). Finally the sections were washed again, mounted with Fluoromount G (Southern Biotechnology Associates, Biozol, Eching, Germany) and stored in the dark at 4°C.

3.5.3 Stereological analysis

The optical disector method was chosen for quantitative analysis because of its efficiancy (Howard and Reed 1998), an important prerequisite when aiming to quantify numerical densities of a variety of cell types in a given brain region (Irintchev et al. 2004a). The method consists of direct counting of objects in relatively thick sections (e.g. 25–50µm) under the microscope using a three-dimensional counting frame ("counting brick" of Howard and Reed, here simply referred to as disector) to "probe" the tissue at random. The base of the frame (dimensions in the x/y plane) is defined by the size of the squares formed by a grid projected into the visual field of the microscope. The height of the disector is a portion of the section thickness defined by two focus planes in the z axis at a distance of x µm. Control of this parameter is achieved by the use of mechanic or electronic devices measuring the movement of the microscope stage in the z axis. Objects (e.g. cells) within each disector are counted according to stereological rules: those entirely within the disector as well as those touching or being disected by the "acceptance", but not the "forbidden" planes of the frame are counted.

The cell counts were performed on an Axioskop microscope equipped with a motorized stage and Neurolucida software controlled computer system (MicroBrightField, Colchester, USA). Sections cut at distances between 3 and 4mm caudally to the rostral pole of the forebrain (where collection of the sections began, see 3.3) were observed under low-power magnification (10 x objective) with a 365/420nm

excitation/emission filter set (01, Zeiss, blue flourescence). The nuclear staining allowed clear distinction of the motor and the sensory cortex (M and S, respectively, in Figure 6) as well as the subdivisions of the hippocampus. For the identification of the substantia nigra pars compacta, an immunohistochemical staining was used.

The viewed area was randomized by setting a reference point at an arbitrary place resulting in an overlay of the visible field by a grid with lines spaced 30µm (substantia nigra) or 60µm (all other areas studied) in both axes. The contours of the area of interest were outlined with the cursor. For the motor and cingulate cortex, layer I was excluded from all measurements because parts of it were sometimes lost together with pieces of pia mater during cutting. Squares within the marked area at distances of 60µm for the substantia nigra and 120µm for the other structures were labeled with a symbol starting from the uppermost left side of the field. A disector depth of 10µm was chosen since antibody penetration was sufficient to enable clear recognition of stained objects within a depth of at least 15µm. The sections were viewed with the 40x magnification objective and 546/590nm excitation/emission filter set (15, Zeiss, red flourescence). The marked meander was scanned and all marked frames were viewed consecutively. Immunolabeled cell profiles that were entirely within the counting frame at any focus level, as well as those attaching to or intercrossed by the forbidden or acceptance lines were marked with a symbol. Then by repeated switching between the red and blue filter sets and changing the focus plane, the nuclei of the labeled cells were identfied. All nuclei that were in focus beyond a guard space (depth 0-2µm from the section surface), i.e. lying within 2 and 12µm below the top of the section, were counted except for those at the "look-up" level (2µm) and such intercrossed by or touching the forbidden lines. Four sections were evaluated bilaterally per animal and staining.

3.5.4 Photographic documentation

Photographic documentation was made on an Axiophot 2 microscope equipped with a digital camera AxioCam HRC and AxioVision software (Zeiss) at highest resolution (2300x2030pixel, RGB). The images were processed using AdobePhotoshop 6.0 software (Adobe Systems Inc., San Jose, California).

3.5.5 Statistical analysis

Statistical analysis was restricted to simple comparisons of mean values of age-matched groups, i.e. littermates, using the two-sided t test for independent groups. A more comprehensive analysis allowing multiple comparisons between groups of different age and genotype appeared unsuitable because of the risk to compare genetically variable (non-littermate) groups separated by several generations in the breeding line. By two or more measurements per parameter and animal, the mean was used as a representative value. Thus, for all comparisons the degree of freedom was determined by the number of animals. The accepted level of significance was 5%.

4 RESULTS

4.1 Morphometric analysis of gross-anatomical variables

4.1.1 Brain mass, volume and specific weight

The brain mass of 2-month-old CHL1-/- animals did not differ from that of CHL1+/+ age matched animals (Figure 7). In older animals, however, a significant difference was present: the average brain mass was larger by 8% and 10% in mutant animals as compared to wild-type control mice at 6 and 12 months of age, respectively (Figure 7).
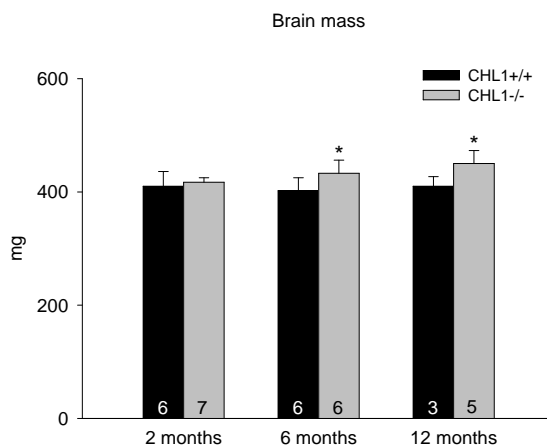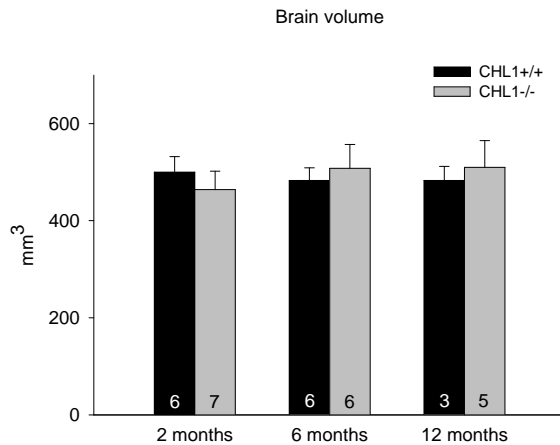

Figure 7: Brain mass of CHL1+/+ (black bars) and CHL1-/- animals (grey bars) studied at the age of 2, 6 and 12 months. Shown are mean values + standard deviation (SD). The numbers in the bars indicate the number of animals per group for which this parameter could be evaluated. Asterisks indicate significant differences as compared to the age-matched group (two-sided t test for independent groups, $p < 0.05$).

The brain volume of CHL1+/+ animals did not differ significantly from that of CHL1-/- mice at all three ages studied (Figure 8). This finding does not necessarily stand in contrast to the observation for brain mass (note similar tendencies for the older age groups). Rather, it reflects a larger experimental error (lower precision of volume as compared to weight measurements, note larger, relative to mean values, standard deviations in Figure 8 in comparison to Figure 7 resulting in failure to detect small differences (below 10%).

Accordingly, the calculated specific weight (mass per unit volume) did not differ between the groups (Figure 9).

Brain volume

Figure 8: Brain volume of CHL1+/+ (black bars) and CHL1-/- animals (grey bars) studied at the age of 2, 6 and 12 months. Shown are mean values + SD. The numbers in the bars indicate the number of animals per group for which this parameter could be evaluated. No significant differences between age-matched groups were found (t test).
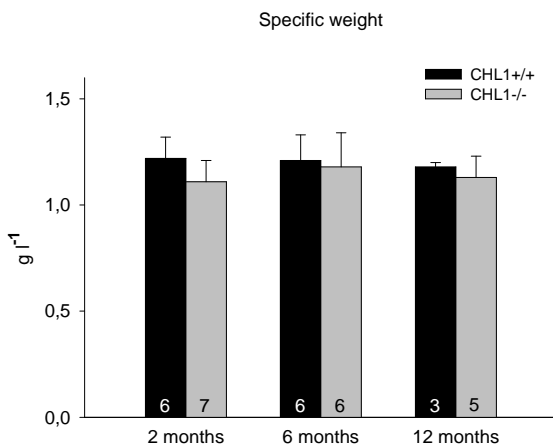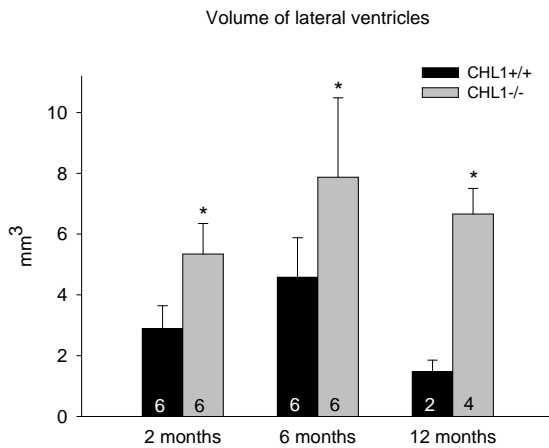

Specific weight

Figure 9: Specific weight of CHL1+/+ (black bars) and CHL1-/- animals (grey bars) studied at the age of 2, 6 and 12 months. Shown are mean values + SD. The numbers in the bars indicate the number of animals per group for which this parameter could be evaluated. No significant differences between age-matched groups were found (t test).

4.1.2 Ventricular volume

Pure observation of spaced-serial sections stained with cresyl violet–Luxol Fast Blue already pointed out that brain ventricles (lateral and third) are larger in CHL1-/- mice compared to CHL1+/+ animals at all ages studied. The differences, however, did not appear to be very large. Estimates of the total ventricular volume using the Cavalieri method on the other hand revealed considerable ventriculomegalia in mutant animals in all age groups (Figure 10 and Figure 11). The increase of the mean lateral and third ventricular volume in mutants compared to wild type mice at 2 and 6 months of age was within the range of 72%-110%. The difference at 12 months was very large (350–625% increase) but since only 2 brains from CHL1+/+ mice could be analyzed and these

appeared to have unusually small ventricles (Figure 10 and Figure 11), this might not be representative. For the size of the lateral ventricles (Figure 10) the total bilateral volume is given. We also studied the ventricular asymmetry by comparing the volume of the left and right lateral ventricle in individual animals (data not shown). No genotype-specific differences were found.

Figure 10: Bilateral volume of lateral brain ventricles in CHL1+/+ (black bars) and CHL1-/- animals (grey bars) studied at the age of 2, 6 and 12 months. Shown are mean values + SD. The numbers in the bars indicate the number of animals per group for which this parameter could be evaluated. Asterisks indicate significant differences as compared to the age-matched group (t test).
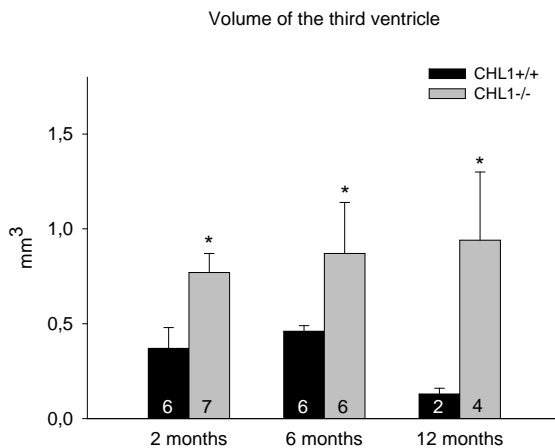
Figure 11: Volume of the third brain ventricle in CHL1+/+ (black bars) and CHL1-/- animals (grey bars) studied at the age of 2, 6 and 12 months. Shown are mean values + SD. The numbers in the bars indicate the number of animals per group for which this parameter could be evaluated. Asterisks indicate significant differences as compared to the age-matched group (t test).

4.1.3 Cortical thickness of motor and cingulate area

The normalized cortical thickness, calculated as the ratio of the cortical segment area (excluding layer I) to the length of the surface (meningeal) boundary of the segment, was similar in the two genotype groups at all ages studied, both in the motor

cortex (Figure 12) and the cingulate cortical area (Figure 13). This finding is important with regard to the interpretation of differences in cell densities (see 4.3).
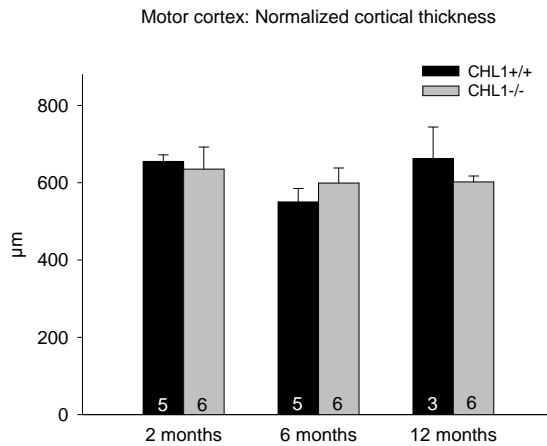
Figure 12: Normalized thickness of the motor cortex in CHL1+/+ (black bars) and CHL1-/- animals (grey bars) studied at the age of 2, 6 and 12 months. Shown are mean values + SD. The numbers in the bars indicate the number of animals per group for which this parameter could be evaluated. No significant differences between age-matched groups were found (t test).

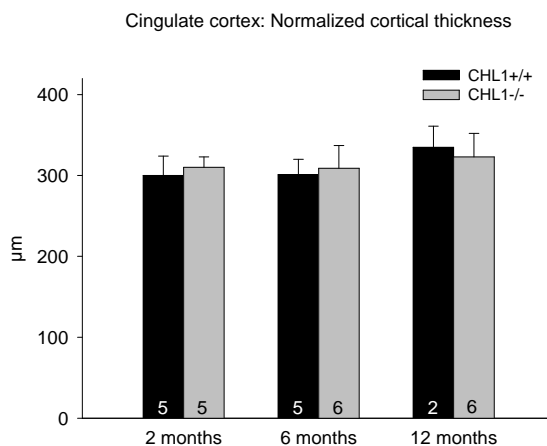**Figure 13:** Normalized thickness of the cingulate cortex in CHL1+/+ (black bars) and CHL1-/- animals (grey bars) studied at the age of 2, 6 and 12 months. Shown are mean values + SD. The numbers in the bars indicate the number of animals per group for which this parameter could be evaluated. No significant differences between age-matched groups were found (t test).

4.1.4 Volume of the Hippocampus

The estimation of the total volume of the hippocampal formation and its subdivisions using the Cavalieri method was not possible because parts of sections containing the ventral hippocampus and the temporo-occipital cortex were lost while cutting in the cryostat. As an alternative, the cross-sectional area of the structures was measured in three spaced-serial sections (250μm apart) from the dorsal hippocampus cut at defined levels (see Materials and methods). The values of the three sections were averaged to reduce errors due to the inevitable, though small, deviations from the "perfect" plane of cutting and rostro-caudal distance from bregma. Since spacing

between the evaluated sections was equal and relatively large (250µm), the area estimates are proportional to the volume of a significant portion of the dorsal hippocampus.

All measurements were performed bilaterally and evaluated separately for the left and right hippocampus. Since the results for the left and the right hippocampus and the degree of asymmetry were similar with respect to genotype-related differences, for clarity and brevity the averaged bilateral values are presented here.

The total area of the hippocampus (Figure 14) and the area of the granular layer of the dentate gyrus (Figure 15) were similar in all age-matched groups indicating a normal size of these structures in mutant animals. The area of the pyramidal layer (CA1-3 areas), however, was significantly larger (+18%) in CHL1-/- animals as compared to CHL1+/+ animals at 2 and 6 months of age (Figure 16) The difference between the mean values of the two groups studied at 12 months of age was not statistically significant but the same tendency seen in younger animals was present ($p < 0.08$, t test, note small number of animals studied per group). The same results were obtained when the area of the pyramidal layer was normalized to the total hippocampal area (Figure 17).

Figure 14: Total cross-sectional area of the hippocampus in coronal brain sections of CHL1+/+ (black bars) and CHL1-/- animals (grey bars) studied at the age of 2, 6 and 12 months. Shown are averaged bilateral mean values + SD. The numbers in the bars indicate the number of animals per group for which this parameter could be evaluated. No significant differences between age-matched groups were found (t test).
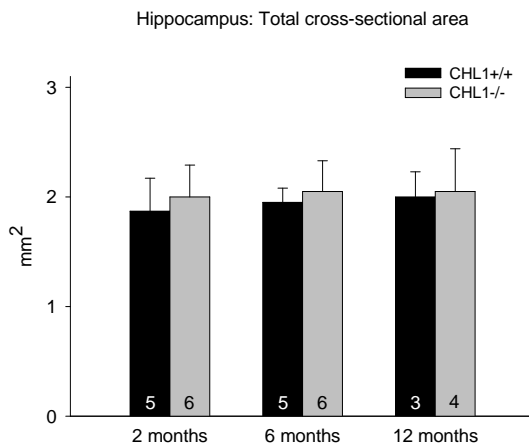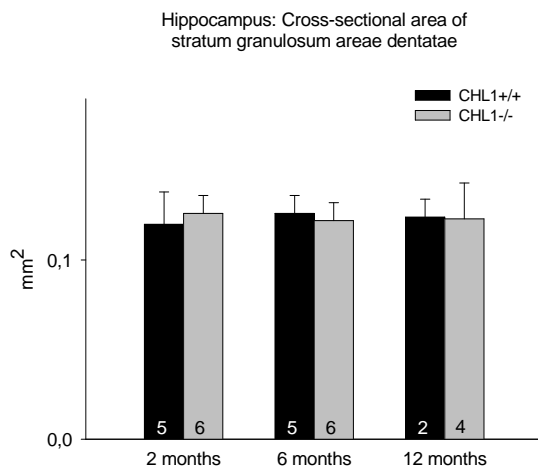
Hippocampus: Cross-sectional area of
stratum granulosum areae dentatae

CHL1+/+
CHL1-/-

Figure 15: Cross-sectional area of the granular layer in the dentate gyrus in coronal brain sections of CHL1+/+ (black bars) and CHL1-/- animals (grey bars) studied at the age of 2, 6 and 12 months. Shown are averaged bilateral mean values + SD. The numbers in the 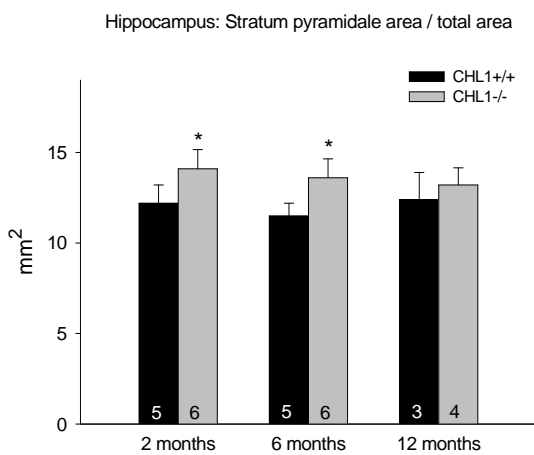bars indicate the number of animals per group for which this parameter could be evaluated. No significant differences between age-matched groups were found (t-test).

Hippocampus: Cross-sectional area of
stratum pyramidale hippocampi
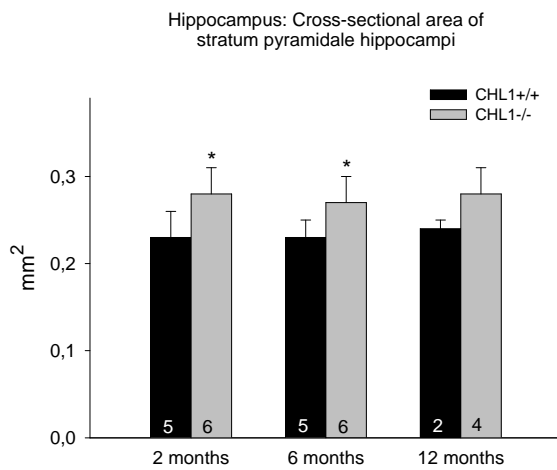
CHL1+/+
CHL1-/-

Figure 16: Cross-sectional area of the pyramidal cell layer in coronal brain sections of CHL1+/+ (black bars) and CHL1-/- animals (grey bars) studied at the age of 2, 6 and 12 months. Shown are averaged bilateral mean values + SD. The numbers in the bars indicate the number of animals per group for which this parameter could be evaluated. Asterisks indicate significant differences as compared to the age-matched group (t test).

Hippocampus: Stratum pyramidale area / total area

CHL1+/+
CHL1-/-

Figure 17: Cross-sectional area of the pyramidal cell layer as a fraction of the total hippocampal area in coronal brain sections of CHL1+/+ (black bars) and CHL1-/- animals (grey bars) studied at the age of 2, 6 and 12 months. Shown are averaged bilateral mean values + SD. The numbers in the bars indicate the number of animals per group for which this parameter could be evaluated. Asterisks indicate significant differences as compared to

the age-matched group (t test).change.

4.2 Immunohistochemical markers, quality of staining and qualitative observations in CHL1+/+ and CHL1-/- animals

For each particular antigen, all sections were stained in the same primary and secondary antibody solutions kept in staining jars and stabilized in order to enable repeated long-term usage (Sofroniew and Schrell 1982; Irintchev et al. 2004a). The previously documented reproducibility of this staining technique was also apparent in this study: the quality of staining remained constant for all batches of slides processed over a period of several months, an important prerequisite for quantitative studies on a large number of animals. No qualitative differences between CHL1+/+ and CHL1-/- animals were noticed in the staining patterns for the detected antigens. Examples of the stainings are shown in Figure 18.
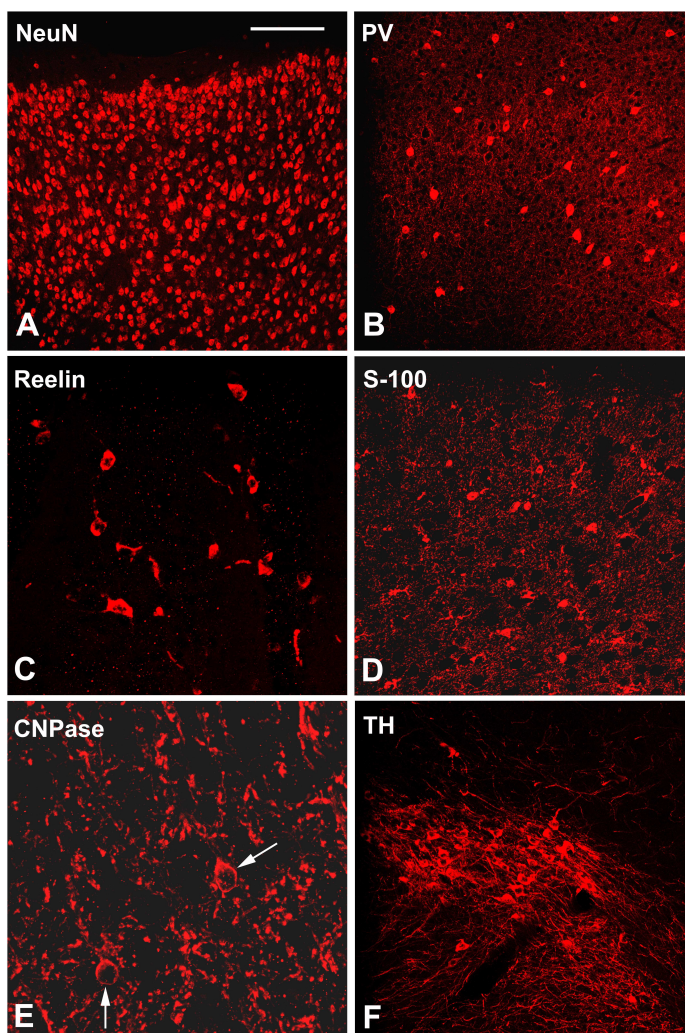
Figure 18: Examples of immunohistochemical stainings in sections of CHL1-/- (A,C,E,F) and CHL1+/+ (B,D) animals. A: NeuN+ cells in the cingulate cortex of a 12-month-old animal; B: PV+ interneurons in the motor cortex of a 6-month-old mouse; C: reelin+ interneurons, hilus of the hippocampus of a 2-month-old animal; D: S-100+ astrocytes, motor cortex of a 2-month-old animal; E: CNPase+ cell bodies (arrows), motor cortex of a 6-month-old animal; F: TH+ neurons in the substantia nigra of a 6-month-old animal. Scale bar in A indicates 100 µm for A,B and F, 50 µm for C and D, and 25 µm for E.

4.3   Stereological analysis of the motor cortex

4.3.1 General observations

Pure observation of cresyl violet-Luxol Fast Blue stained sections revealed an apparently normal structure of the motor cortex with the typical arrangement of cells in six layers. Also with regard to distribution patterns of immunocytochemically identified cells (see 4.3.3-4.3.7) no differences between CHL1-/- and CHL1+/+ animals were detected.

4.3.2 Total cell density

The nuclear staining was used to estimate the numerical density (i.e. number per unit volume) of all cells as a reference value indicative of global alterations in the motor cortex. While no difference between 2-month-old CHL1+/+ and CHL1-/- animals was found, the total cell density in the cortex of 6-and 12-month-old mutant animals was significantly lower compared to age-matched control animals (-11%, Figure 19) indicating age-dependent changes in the total cell population in the CHL1 deficient motor cortex. With respect to these differences it is important to note that the cortical thickness was similar in wild-type and mutant animals at all ages studied. Therefore, the differences in the estimates of the total cell density reflect differences in the absolute number of cells in a cortical column (cell number under unit of cortical surface).
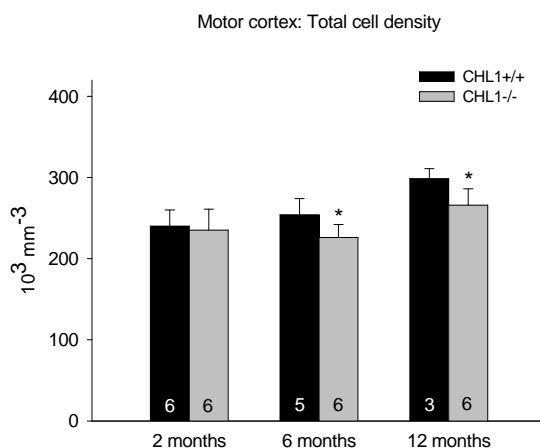
Figure 19: Numerical density of the total cell population, identified by nuclear staining, in the motor cortex of CHL1+/+ (black bars) and CHL1-/- animals (grey bars) studied at the age of 2, 6 and 12 months. Shown are mean values + SD. The number of animals studied per group is indicated at the base of each bar. Asterisks indicate significant differences as compared to the age-matched group (*t* test).

4.3.3 Total neuronal population

In contrast to the age-related and genotype-specific dynamics in the total cell population, the density of all neurons (NeuN-positive) in the motor cortex of CHL1+/+ and CHL1-/- mice was similar at all ages studied (Figure 20).
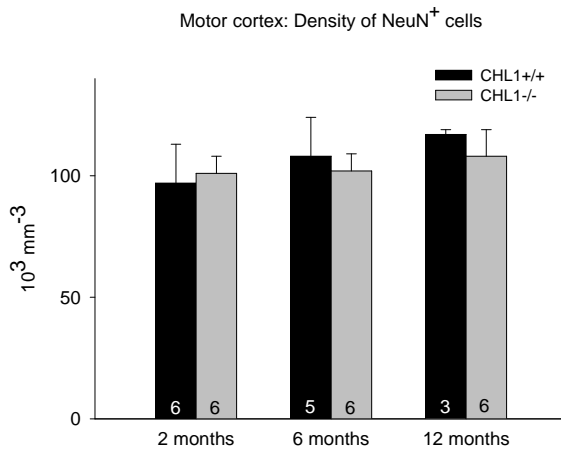
Figure 20: Numerical density of the total neuronal population in the motor cortex of CHL1+/+ (black bars) and CHL1-/- animals (grey bars) studied at the age of 2, 6 and 12 months. Shown are mean values + SD. The number of animals studied per group is indicated at the base of each bar. No significant differences between age-matched groups were found (t test).

4.3.4 Parvalbumin-positive interneurons

A large (+35%) and statistically significant difference was found in the number of PV-positive interneurons in mutant animals compared to wild-type control animals at the age of 2 months (Figure 21). The densities in all older groups were similar.
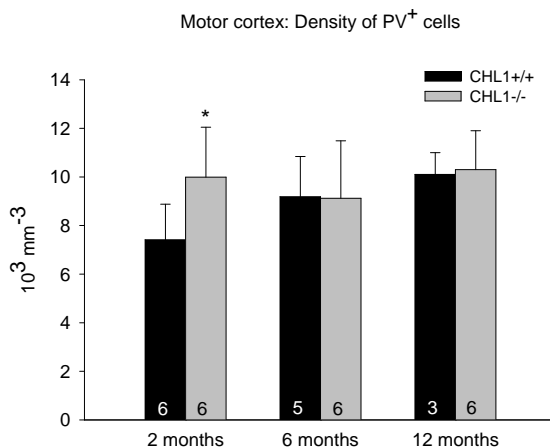
Figure 21: Numerical density of PV-positive interneurons in the motor cortex of CHL1+/+ (black bars) and CHL1-/- animals (grey bars) studied at the age of 2, 6 and 12 months. Shown are mean values + SD. The number of animals studied per group is indicated at the base of each bar. Asterisks indicate significant differences as compared to the age-matched group (t test).

4.3.5 Reelin-positive interneurons

Lower numbers of reelin-positive cells were found in CHL1-/- animals compared to CHL1+/+ mice at all ages studied (-20%, Figure 22).

Figure 22: Numerical density of reelin-positive interneurons in the motor cortex of CHL1+/+ (black bars) and CHL1-/- animals (grey bars) studied at the age of 2, 6 and 12 months. Shown are mean values + SD. The number of animals studied per group is indicated at the base of each bar. Asterisks indicate significant differences as compared to the age-matched group (t test).

4.3.6 Astrocytes and oligodendrocytes

The estimation of numerical densities of S-100-positive astrocytes (Figure 23) and CNPase-positive oligodendrocytes (Figure 24) revealed no significant differences between mutant and wild-type control animals at any age indicating that CHL1 deficiency does not have an impact on these glial cell types. Furthermore, the normal numbers of astrocytes in CHL1-/- animals at 2, 6 and 12 months of age suggest an absence of neurodegenerative processes associated with astrogliosis.
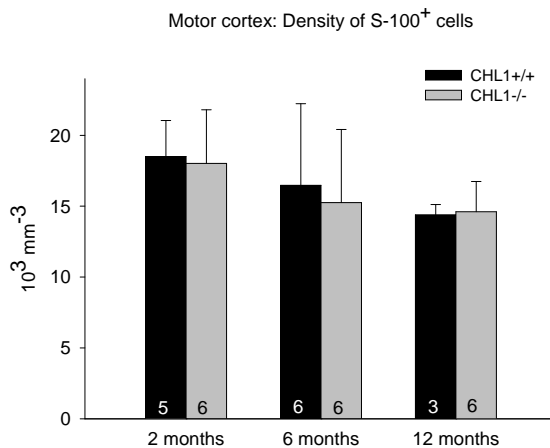
Figure 23: Numerical density of S-100-positive astrocytes in the motor cortex of CHL1+/+ (black bars) and CHL1-/- animals (grey bars) studied at the age of 2, 6 and 12 months. Shown are mean values + SD. The number of animals studied per group is indicated at the base of each bar. No significant differences between age-matched groups were found (t test).
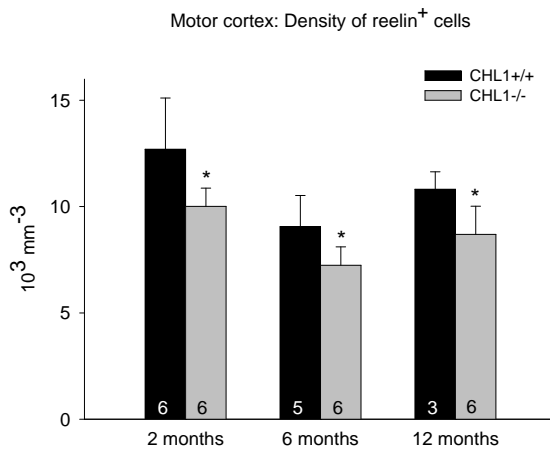
Motor cortex: Density of CNPase$^+$ cells
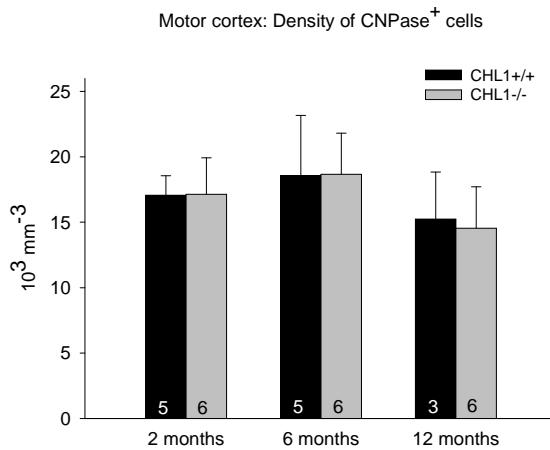
Figure 24: Numerical density of CNPase-positive oligodendrocytes in the motor cortex of CHL1+/+ (black bars) and CHL1-/- animals (grey bars) studied at the age of 2, 6 and 12 months. Shown are mean values + SD. The number of animals studied per group is indicated at the base of each bar. No significant differences between age-matched groups were found (*t* test).

4.3.7 Microglia

Iba1, a recently discovered protein, is involved in the activation of microglia and thus expressed in quiescent cells (Imai and Kohsaka 2002). Following activation, the protein expression is enhanced and maintained at high level in active cells. This allows reliable identification of both resting and activated microglial cells.

The results of the quantitative analysis of Iba1-positive cells revealed a largely increased number of microglial cells in 2-month-old CHL1-/- animals as compared to control animals (+45%) (Figure 25). No differences between the matched groups were present at 6 and 12 months of age.

Motor cortex: Density of Iba1$^+$ cells

Figure 25: Numerical density of Iba1-positive microglial cells in the motor cortex of CHL1+/+ (black bars) and CHL1-/- animals (grey bars) studied at the age of 2, 6 and 12 months. Shown are mean values + SD. The number of animals studied per group is indicated at the base of each bar. Asterisks indicate significant differences as compared to the age-matched group (*t* test).
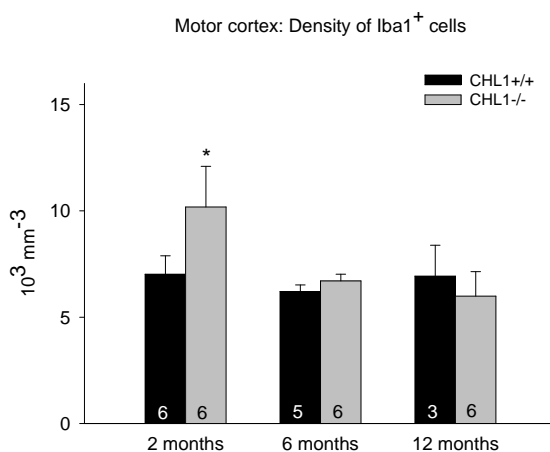
The abnormally high number of microglial cells in 2-month-old CHL1-/- animals was surprising with regard to the normal number of astrocytes in the same animals (see 4.3.6). It appeared that either neuronal cell death and reactive microgliosis without astroglial activation have occured or that the high number of microglial cells is not related to neuronal cell death. To resolve this issue, the morphology and distribution of Iba1-positive cells were analyzed in sections of 2-month-old CHL1-/- and CHL1+/+ animals (Figure 26). The morphology of microglial cells changes after activation (reactive microglia): the size of the cell body is enlarged and the slender cell processes become thicker, shorter and can even disappear completely in phagocytic microglia (Streit et al. 1999). While resting microglial cells are evenly distributed throughout the tissue mostly as single cells, activated cells form aggregates in areas of cell death. Both signs of activation of single Iba1 positive cells and clusters were seen in CHL1-/- as well as in CHL+/+ animals but in both phenotypes these phenomena were extremely rare: occasionally a few "events" could be detected if the whole coronal section, containing thousands of microglial cell profiles, was most carefully scanned at 40x magnification. These observations suggest that massive cell death does not occur in CHL1-/- animals at 2 months of age.
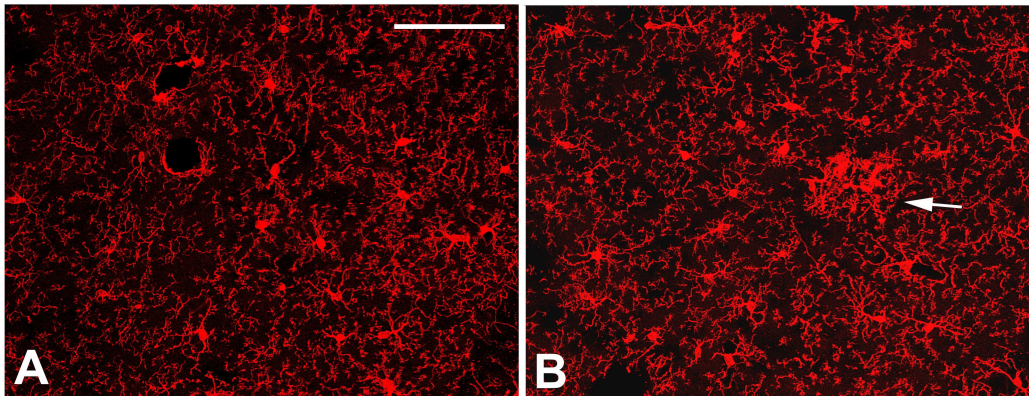
Figure 26: Iba1+ microglial cells in the stratum radiatum of the CA1 hippocampal field of a CHL1+/+ mouse (A) and a CHL1-/- animal (B). Arrow in B indicates a cluster of microglial cells. Scale bar in A indicates 100µm for both panels.

4.4 Stereological analysis of the cingulate cortex

The cell populations analyzed in the motor cortex (M1-M2) were also studied in the adjacent cingulate areas designated as Cg1-Cg2 (Franklin and Paxinos 1997). The results are shown in Figure 27, Figure 28, Figure 29, Figure 30, Figure 31 and Figure 32. In contrast to the motor area, no significant differences between CHL1-/- and CHL1+/+ animals were found for any cell type at any age studied. These results indicate that functionally different cortical regions may be affected in a different way by the constitutive absence of CHL1. With respect to this notion one finding in the cingulate cortex should be pointed out: the number of reelin-positive interneurons was, though not significantly, consistently higher in the mutants at all ages (17–19% increase, see Figure 30 and compare with the deficit of reelin interneurons in the motor cortex at of mutants at all ages, Figure 22).
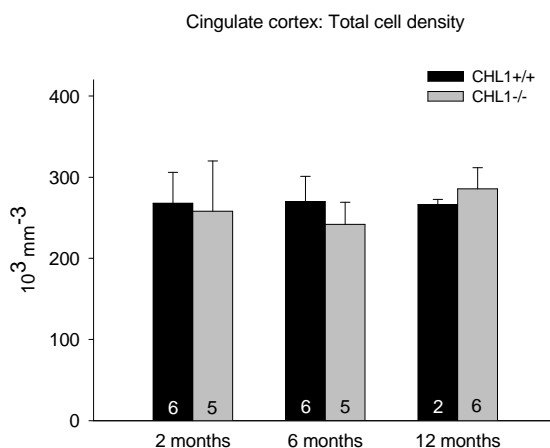
Figure 27: Numerical density of the total cell population, identified by nuclear staining, in the cingulate cortex of CHL1+/+ (black bars) and CHL1-/- animals (grey bars) studied at the age of 2, 6 and 12 months. Shown are mean values + SD. The number of animals studied per group is indicated at the base of each bar. No significant differences between age-matched groups were found (*t* test).
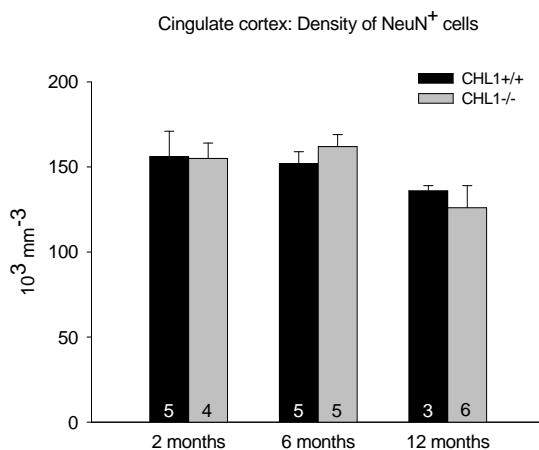
Figure 28: Numerical density of the total neuronal population in the cingulate cortex of CHL1+/+ (black bars) and CHL1-/- animals (grey bars) studied at the age of 2, 6 and 12 months. Shown are mean values + SD. The number of animals studied per group is indicated at the base of each bar. No significant differences between age-matched groups were found (*t* test).

Cingulate cortex: Density of PV$^+$ cells
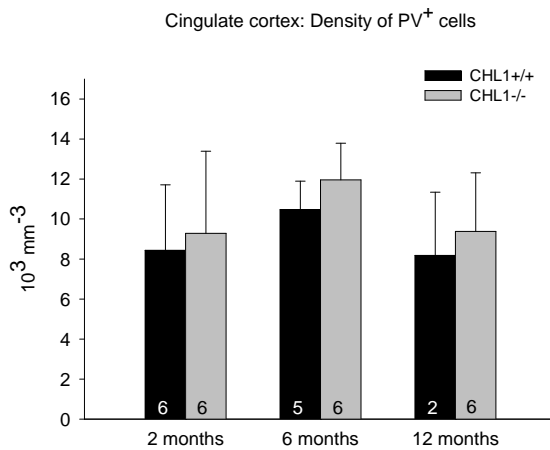
Figure 29: Numerical density of PV-positive interneurons in the cingulate cortex of CHL1+/+ (black bars) and CHL1-/- animals (grey bars) studied at the age of 2, 6 and 12 months. Shown are mean values + SD. The number of animals studied per group is indicated at the base of each bar. No significant differences between age-matched groups were found (*t* test).

Cingulate cortex: Density of reelin$^+$ cells
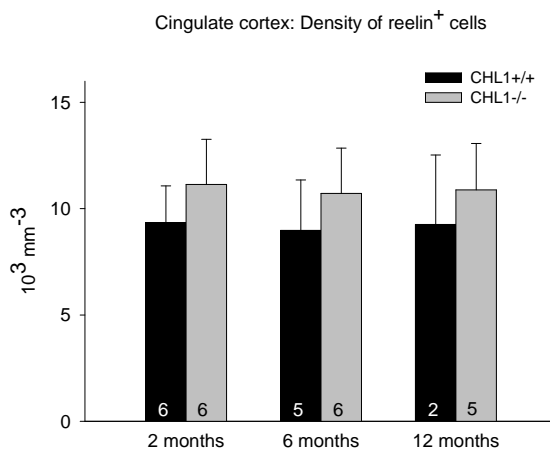
Figure 30: Numerical density of reelin-positive interneurons in the cingulate cortex of CHL1+/+ (black bars) and CHL1-/- animals (grey bars) studied at the age of 2, 6 and 12 months. Shown are mean values + SD. The number of animals studied per group is indicated at the base of each bar. No significant differences between age-matched groups were found (*t* test).

Cingulate cortex: Density of S-100$^+$ cells

Figure 31: Numerical density of S-100-positive astrocytes in the cingulate cortex of CHL1+/+ (black bars) and CHL1-/- animals (grey bars) studied at the age of 2, 6 and 12 months. Shown are mean values + SD. The number of animals studied per group is indicated at the base of each bar. No significant differences between age-matched groups were found (*t* test).

Cingulate cortex: Density of Iba1$^+$ cells

Figure 32: Numerical density of Iba1-positive microglial cells in the cingulate cortex of CHL1+/+ (black bars) and CHL1-/- animals (grey bars) studied at the age of 2, 6 and 12 months. Shown are mean values + SD. The number of animals studied per group is indicated at the base of each bar. No significant differences between age-matched groups were found (*t* test).

4.5 Stereological analysis of the hippocampus

The hippocampus was not analyzed as thoroughly as the cortical areas. Evaluated were three cell types, PV-and reelin-positive interneurons and microglia, for which differences were found in the motor cortex. An age-related dynamics similar to the motor cortex was found for PV-and Iba1-positive cells. In CHL1-/- animals, PV interneurons, normal in number at 2 months, declined to about 80% of the values of CHL1+/+ mice at 6 and 12 months of age (Figure 33). The density of microgial cells in CHL1-/- animals was abnormally high at 2 months of age (+38% versus CHL1+/+ animals), but normal at 6 and 12 months (Figure 35). The CHL1 deficiency did not appear to affect the reelin interneurons in the hippocampus (Figure 34), compare with the deficit at all ages in the motor cortex, (Figure 22). These findings indicate again that the mutation affects the brain in a region-specific manner (see also 4.4).

Hippocampus: Density of PV$^+$ cells
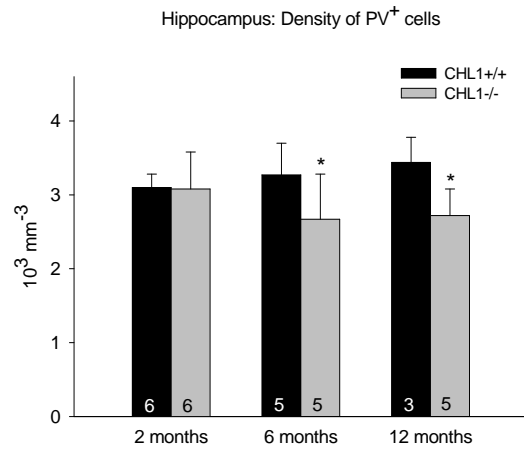
Figure 33: Numerical density of PV-positive interneurons in the hippocampus of CHL1+/+ (black bars) and CHL1-/- animals (grey bars) studied at the age of 2, 6 and 12 months. Shown are mean values + SD. The number of animals studied per group is indicated at the base of each bar. Asterisks indicate significant differences as compared to the age-matched group (*t* test)

Hippocampus: Density of Reln$^+$ cells
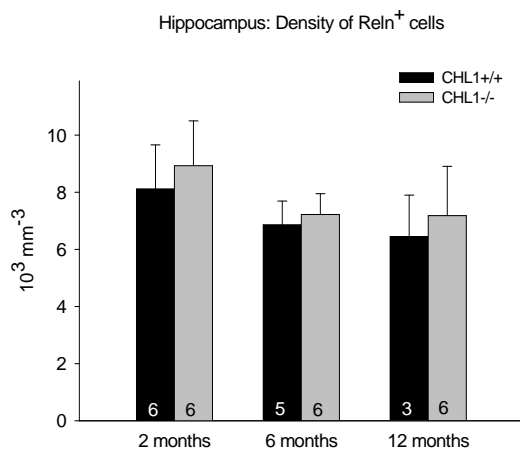
Figure 34: Numerical density of reelin-positive interneurons in the hippocampus of CHL1+/+ (black bars) and CHL1-/- animals (grey bars) studied at the age of 2, 6 and 12 months. Shown are mean values + SD. The number of animals studied per group is indicated at the base of each bar. No significant differences between age-matched groups were found (*t* test).
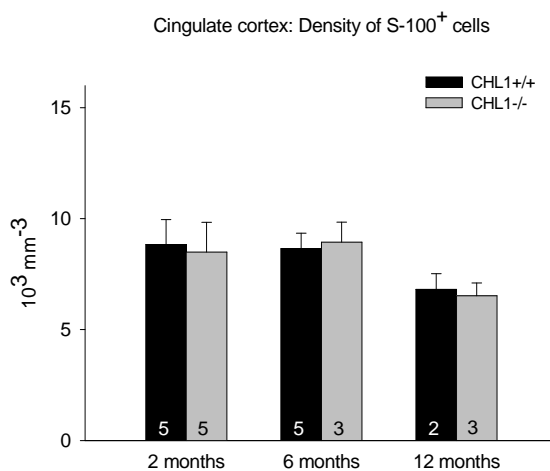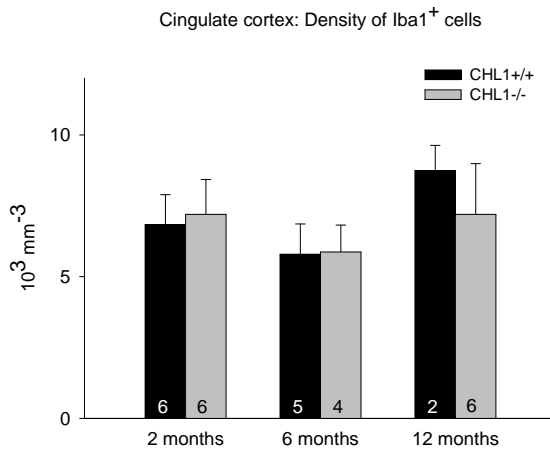
Hippocampus: Density of Iba1$^+$ cells
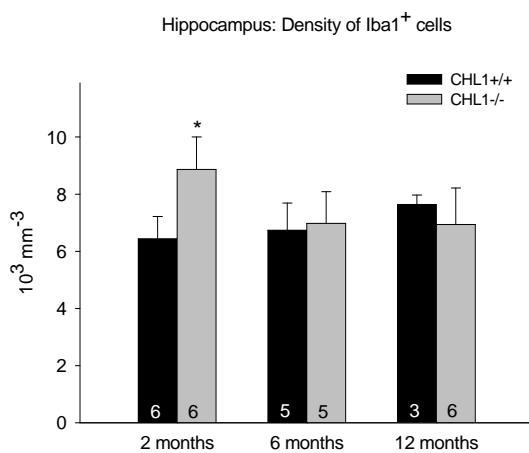
Figure 35: Numerical density of Iba1-positive microglial cells in the hippocampus of CHL1+/+ (black bars) and CHL1-/- animals (grey bars) studied at the age of 2, 6 and 12 months. Shown are mean values + SD. The number of animals studied per group is indicated at the base of each bar. Asterisks indicate significant differences as compared to the age-matched group (*t* test).

4.6 Stereological analysis of the substantia nigra

To get an insight into the structural integrity of the dopaminergic system, the density of TH-positive neurons was evaluated in the substantia nigra pars compacta. These neurons are dopaminergic and project primarily to the striatum. Like for other neuronal cell types, also in the substantia nigra an age-related loss of cells (around 25%) was found in CHL1-/- animals between the age of 2 and 6 months (Figure 36).
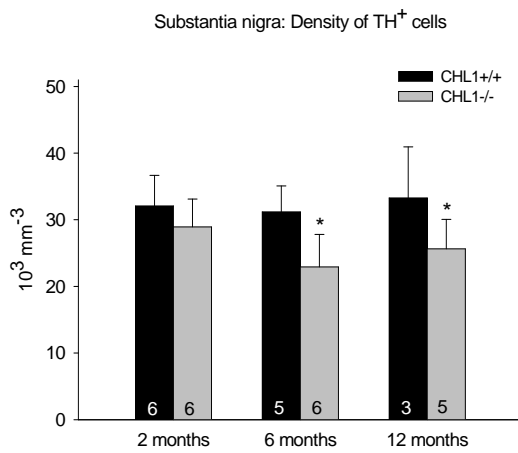
Figure 36: Numerical density of TH-positive neurons in the substantia nigra of CHL1+/+ (black bars) and CHL1-/- animals (grey bars) studied at the age of 2, 6 and 12 months. Shown are mean values + SD. The number of animals studied per group is indicated at the base of each bar. Asterisks indicate significant differences as compared to the age-matched group (*t* test).

5 DISCUSSION

The results of this study show that deficient expression of the cell recognition molecule CHL1 in the mouse causes a range of abnormalities in different brain regions. Apart from discrete gross structural malformations, subpopulations of inhibitory cells and dopaminergic neurons are affected in an age-dependent and brain region-specific manner.

	2 months	6 months	12 months
Gross anatomical variables			
Brain Mass	=	↑	↑
Lateral ventricular volume	↑	↑	↑
Third ventricular volume	↑	↑	↑
Area of CA pyramidal cell layer	↑	↑	=
Stereological analysis (Motor			
Total cell density	=	↓	↓
PV-density	↑	=	=
Reelin-density	↓	↓	↓
Iba1-density	↑	=	=
Stereological analysis (Cingulate			
Total cell density	=	=	=
PV-density	=	=	=
Reelin-density	=	=	=
Iba1-density	=	=	=
Stereological analysis (Hippocampus)			
PV-density	=	↓	↓
Reelin-density	=	=	=
Iba1-density	↑	=	=
Stereological analysis (Substantia			
TH-density	=	↓	↓

Table 3: Summary of differences found comparing CHL1-/- and CHL1+/+ mice in different brain regions and at different ages. Arrows indicate significantly lower ↓ or higher ↑ values in mutant animals as compared to control animals, = indicates that there is no significant difference.

5.1 Morphological aberrations in the CHL1 deficient mouse

An overview of the most important results of this study is given in Table 3. Not included in this table are variables for which no differences between the mutant and the wild-type animals were found in any region and at any age studied (brain volume, cortical thickness, cross-sectional areas of the hippocampus and the granule cell layer of the dentate gyrus, densities of NeuN$^+$, CNPase$^+$ and S-100$^+$ cells).

5.1.1 Gross morphological variables

Previous qualitative evaluations of major brain regions have not revealed any severe abnormalities in the CHL1 deficient mouse (Montag-Sallaz et al. 2002). The differences between CHL1-/- and CHL1+/+ animals described in the study of Montag-Sallaz and co-workers are rather subtle and include larger ventricles and aberrant projections of hippocampal granule cells and of olfactory neurons. In agreement with these results we found no differences between mutant and wild-type animals in the thickness of the cerebral cortex (motor and cingulate area), the cross-sectional area of the hippocampus and the dentate gyrus. Small differences were found in the total brain mass and the cross-sectional area of the pyramidal cell layer in the hippocampus (around 10% higher values in CHL1-/- animals as compared to CHL1+/+ mice). The most robust aberration in the brains of CHL1 deficient animals is the enormously increased ventricular volume by a factor of two and more as compared to wild-type animals at different ages (see Table 3 and 4.1.2).

The genotype-specific differences in the ventricular volume and the area of the pyramidal cell layer of the hippocampus were found at all three ages studied (Table 3, 4.1.2 and 4.1.4). This was not the case for the brain mass which was found not to be increased in 2-month-old mutants compared to wild type mice but increased by some 10% between 2 and 6 months of age in CHL1-/- animals as compared to CHL1+/+ littermates (Table 3 and 4.1.1). This finding is of importance since it indicates abnormal postnatal dynamics of a global structural brain variable. Moreover, recent studies have shown that the brain of mutant animals is even smaller than that of control wild-type animals at the age of one month (-10%, Irintchev, not published). Thus, it appears that the CHL1-/- mutation causes a deficiency in the total brain mass during embryonic/early postnatal development which is "overcompensated" during later postnatal stages.

5.1.2 Stereological data

The comprehensive stereological analysis of a variety of cell types provides a large and novel data set with regard to the cellular composition of different brain regions in wild-type animals. These data are of general interest since such information, derived from simultaneous analysis of major cell types in the CNS, cannot be found in the literature. The only exception is a recent study on the cerebral cortex of tenascin-C deficient and non-deficient mice performed in our laboratory (Irintchev et al. 2004a). The present results on various numerical densities in the motor cortex of wild-type animals are in good accordance with the results of the previous investigation indicating the reproducibility of this quantitative approach. Beyond producing data of general interest, we could identify a number of genotype-specific differences in cell densities which require special attention (see 5.1.2.2).

5.1.2.1 Cell populations unaffected by the mutation in the CHL1 gene

The numerical densities of NeuN$^+$ neurons, S-100$^+$ astrocytes and CNPase$^+$ oligodendrocytes were studied in the motor and cingulate cortex and no differences between CHL1-/- and CHL1+/+ animals were found. This could be interpreted as a hint that CHL1 expression in neurons and astrocytes, as well as oligodendrocyte precursors during development, and in many brain regions also during adulthood (Hillenbrand et al. 1999), is dispensable for the formation and maintenance of these major cellular populations. A conclusion like this appears, however, superficial. In this study we have evaluated a single variable with regard to these cellular populations namely the cell number. Other aspects such as functional cell properties, neuronal connectivity, dendritic tree morphologies and dendritic spine densities, which might be substantially altered as a result of the gene mutation, were not addressed in this study. In fact, the finding of reduced numbers of inhibitory neurons (see Table 3 and 5.1.2.2) is a hint that CHL1 is essential for the maintenance of particular neuronal subpopulations and the finding is consistent with results showing that CHL1 promotes neuronal survival (Chen et al. 1999). Furthermore, a recent study has identified a role for CHL1 in area-specific migration and dendrite guidance of pyramidal neurons: in CHL1 knockout mice pyramidal neurons in layer V of the visual cortex are deeply displaced and have inverted polarity, while neurons in the somatosensory cortex develop misoriented apical dendrites (Demyanenko et al. 2004).

5.1.2.2 Cell populations affected by the mutation in the CHL1 gene

The PV$^+$ interneurons were more numerous in the motor cortex of 2-month-old CHL1-/- mice (+35%) as compared to CHL1+/+ littermates while the numbers were similar in both genotypes at older ages (Table 3 and 4.3.4). In the hippocampus, the numbers of PV$^+$ cells were similar in mutant and wild-type animals at the age of two months but significantly lower (-20%) in CHL1-/- mice at 6 and 12 months of age (Table 3 and 4.5). Thus, both in the motor cortex and the hippocampus there is an age-related decline in the numbers of PV$^+$ interneurons in CHL1-/- mice as opposed to CHL1+/+ animals. This finding is further supported by results of a recent study on the hippocampus of 1-month-old CHL1 deficient mice in which a surplus of about 90% PV$^+$ cells has been found compared to non-deficient control animals (Nikonenko AG, Sun M, Irintchev A, Dityatev A, Schachner M, unpublished observations). In the cingulate cortex no age-related decline was observed, on the contrary there was a tendency for higher numbers of PV$^+$ cells in mutant animals (~15%) at 6 and 12 months of age (Table 3 and 4.4.). These findings indicate that the loss of PV$^+$ interneurons is a phenomenon affecting specific regions of the brain rather than being a "global" phenomenon in the CHL1 deficient brain.

The PV$^+$ interneurons comprise a major proportion of GABAergic cells in the hippocampus and cerebral cortex (Fukuda and Kosaka 2000; Galarreta and Hestrin 2002; Freund 2003). These inhibitory neurons are coupled by both chemical and electrical synapses and form an inhibitory network which operates at high-frequency discharge rates. This network has a strong impact on neuronal excitability and, thus, regulates basic physiological properties such as synchronization and oscillatory activities in the hippocampus and in the cortex. Therefore, changes in the PV$^+$ interneuron-mediated inhibition have profound effects on hippocampal and cortical function and have been implicated in schizophrenia (see 5.3.2.2).

Alterations in the numbers of reelin-immunoreactive interneurons in specific brain regions have, in addition to PV$^+$ cells, also been observed in schizophrenic patients (see 5.3.2.2). Our study revealed a significant reduction of this cell type in CHL1-/- animals (-20%) as compared to CHL1+/+ animals in the motor cortex at all ages studied (Table 3 and 4.3.5). In contrast to the motor cortex, no differences were found in the hippocampus and a tendency for higher numbers in mutant animals was found in the cingulate cortex at all ages studied (Table 3, 4.4 and 4.5). Therefore, for this cell type gene defect-related alterations also affected specific brain regions.

Total cell density also appeared to be affected in a region-and age-related manner: a decline was found in the motor cortex between 2 and 6 months in mutant animals while no differences between CHL1-/- and CHL1+/+ mice were found in the cingulate cortex (Table 3, 4.3.2 and 4.4). These findings indicate, in conjunction with the changes seen for other cell types, that the motor cortex is a "target" of abnormal postnatal dynamics of cell populations while the cingulate cortex appears to be spared.

Abnormally high numbers of Iba1 positive microglial cells were found in 2-month-old CHL1-/- animals in the motor cortex and in the hippocampus, but not in the cingulate cortex (Table 3, 4.3.7, 4.5, 4.4). At older ages the numbers in the CHL1-/- mice were similar to those in CHL1+/+ animals in all brain regions.

Thus, the changes in the microglial population must be related to the loss of inhibitory interneurons: larger numbers of Iba1 positive cells were present in affected areas and at an age (2 months) at which PV^+ neuronal numbers were still normal (hippocampus) or higher than normal (motor cortex, see Table 3). Despite increased microglial cell density in CHL1 mutant animals at 2 months of age (Table 3, 4.3.7, 4.5, 4.4), no apparent morphological signs of microglial cell activation or massive cell death were observed. This is in accordance with the absence of astrogliosis (normal number of S100 positive neurons in mutants as compared to wild type littermates) but raises the question of what the reason for the high number of microglial cells is. A plausible explanation would be that this is a moderate reactive microgliosis caused by death of inhibitory neurons which only account for a minor proportion of all neurons, occurring at a slow rate over an extended time-period. Another intriguing possibility is that the phenomenon is related to an abnormal turn-over rate of synapses, a speculation based on the known function of microglial cells in synapse elimination in motor nuclei after peripheral nerve injury ("synaptic stripping", Moran and Graeber 2004).

5.2 Insufficiencies of current animal models of schizophrenia

So far, studies on animals have had little impact on the diagnosis and treatment of schizophrenia as opposed to hypertension or diabetes models, for example (Kilts 2001). This clearly indicates that more relevant models are urgently needed to increase the

perspective for a better understanding of the disease`s pathophysiology and for a rather causal treatment of the illness.

The modern view of neuroscience is that clinically relevant psychiatric conditions have a primary dysfunction of neuronal systems at their origin (Cowan et al. 2000). Since disruption in neuronal circuitries and functions can affect both human and animal behavior in a similar way the use of animal models would allow to manipulate candidate causal factors and invasively explore the consequences of such manipulations. These are investigative strategies that are highly limited in humans. There are several reasons for the lack of suitable animal models of which the most fundamental is the caveat of faithfully reproducing what is generally perceived to be a cognitive disorder in less cognitively developed animals. Furthermore, heterogeneity in clinical symptoms, varying course of the disorder and multiple potential causative factors represent significant obstacles to the identification and establishment of suitable animal models (Marcotte et al. 2001).

5.2.1 The neurodevelopmental theory

The neurodevelopmental theory of schizophrenia postulates that the pathogenic condition that leads to schizophrenia develops in the middle stage of intrauterine life, long before the onset of symptoms (Weinberger 1987). Damage before this time would affect neurogenesis and thus lead to severe structural and cellular cortical abnormalities, which are not observed in schizophrenia (Harding 1992). CHL1 expression is first detectable in the mouse brain at embryonic day 13 when axonal outgrowth in the CNS starts (Hillenbrand et al. 1999). A lack of CHL1 would therefore be able to produce a pathogenic condition in the middle of intrauterine life potentially leading to schizophrenia. It has been assumed that defects in brain development lead to abnormal neural connectivity between the temporo-limbic and frontal cortices (Wood et al. 1998).

Developmental abnormalities in schizophrenic patients become evident early in life, long before the clinical manifestation of the disease. Observations on children at a high risk to develop schizophrenia, i.e. with a positive family history, have shown that those children who later develop the disease have neurological and motor deficits from infancy on, which continue through school age and adolescence (Niemi et al. 2003). Lower IQ, attention deficits and poorer school and social adjustment are typically found

in children who will develop schizophrenia compared to controls which proves that the pathology must be present before the actual onset of symptoms.

The disorder itself with psychotic symptoms typically appears after puberty which suggests that puberty is a critical maturational period during which a predisposition might, but does not necessarily need to evolve into the disease (Walker et al. 2004). Overproduction and elimination of synapses, receptors and function is the mechanism by which the brain fine-tunes itself in order to achieve its adult topography. The overproduction phase is thought to maximize the information-carrying capacity of the immature brain. With the onset of puberty synaptic efficiancy is streamlined in a regionally specific manner (Andersen 2003; Feinberg 1982; Walker EF 1994).

Developmental abnormalities and an onset after puberty seem to militate in favor of the neurodevelopmental theory with an *early insult* and a delayed manifestation, suggesting an interactive process between deficit and development.

The importance of genetic factors in the etiology of schizophrenia is nowadays beyond doubt and the neurodevelopmental theory has been widely accepted. Schizophrenia seems to involve the interaction of a large number of genes and it is thus unlikely to be faithfully modeled in its entirety by the approach of animal models. Furthermore, environmental factors might play an important role. According to the widely accepted "two-hit hypothesis" (Bayer et al. 1999b, Walker et al. 2004), the mutant gene or rather multiple mutant genes form the basis for the disease ("first hit"). During fetal development an environmental factor ("second hit") leads to a dysfunction of chronic molecular processes by modulating the mutant gene`s function. Studies of cesarean delivery or anoxia in rats have shown increased dopaminergic hyper-responsiveness to psychostimulants (El Khodor and Boska 1998) and stress (Boska et al. 1998) significantly depending on the genetic background of the animal (Berger et al. 2000). Only both hits together trigger the disease process (Bayer et al. 1999b). We postulate that a mutation in the CHL1 gene leads to a dysfunction in brain development being the first hit in the pathogenesis of schizophrenia.

5.2.2 Current animal models

Historically animal models have predominantly focused on alterations of transmitter systems and lesions of defined areas. Up to now it has only been possible to enlighten

certain aspects of the disease without any significant contribution to the understanding of the etiology of schizophrenia.

5.2.2.1 Pharmacological and lesion models

Pharmacological models of schizophrenia are based on the understanding of alterations in various neurotransmitter systems. The best known model is the dopamine model which is based on the idea that a hyperactivity of mesolimbic dopaminergic neurons produces the positive symptoms (Seeman 1987) while a hypodopaminergic state of mesocortical dopaminergic neurons is proposed to be the basis of negative symptoms (Dworkin and Opler 1992). In the animal model the administration of amphetamine and related psychostimulants reliably stimulates behavioral alterations such as hyperlocomotion and stereotypy (Kokkinidis and Anisman 1980) and can be attenuated by treatment with antipsychotics. Prepulse inhibition (PPI), which is a measure of sensorimotor gating is impaired after administration of a dopamine agonist mimicing the PPI deficits observed in schizophrenia (Kokkinidis and Anisman 1980). Pharmacological models like the Dopmine model mimic the symptoms of schizophrenia but do not give the answer to underlying mechanism by which the dopamine activity is altered. There are also models regarding other transmitters such as GABA, serotonin or glutamate following the same principle.

The next step designing an animal model for schizophrenia was the development of a number of targeted lesion models. They typically involve exitotoxic agents which destroy neuronal tissue through stimulation of excitatory glutamate release or by acting as direct glutamate receptor agonists. Regions which are supposed to be involved in the etiology of schizophrenia like the prefrontal cortex, the hippocampus and the thalamus received a great deal of experimental attention. Lesions in these regions result in an enduring hyper-responsiveness to stress (Jaskiw et al.1990), transient increases in locomotor exploration and amphetamine induced stereotypy (Braun et al. 1993).

The principal advantage of neonatal lesion models is the ability to demonstrate a delayed onset of symptoms testing the neurodevelopmental theories of schizophrenia, the drawback of all experimentally induced lesion models is that they reflect far greater damage than what is seen in the brains of schizophrenic patients. Rats with neonatal excitotoxic lesions of the ventral hippocampus showed delayed (post-puberal) onset of increased hyperlocomotion (Lipska et al. 1993), reduced PPI (Swerdlow et al. 1990),

haloperidol-induced catalepsy and enhanced apomorphine induced stereotypies (Lipska and Weinberger 1993).

It is now clear that the pharmacological and lesion animal models have reached the limit of their predictive and explanatory capabilities (Marcotte et al. 2001). More promising appear neurodevelopmental animal models in which epigenetic factors such as neonatal stress or post-weaning social isolation are used to induce schizophrenia-like behaviors (Van den Buuse et al. 2003). In such a model, however, the role of genetic predisposition can not be studied.

5.2.2.2 Genetic models

Over the last years, genetic studies in humans have identified a number of genes as schizophrenia susceptibility factors when mutated (Harrison and Owen 2003). The identified genes display functions that fit with the neurodevelopmental hypothesis for schizophrenia. Among these genes is Disrupted-in-SChizophrenia 1 (DISC1) which is prominently expressed in the developing nervous system and has been found to be mutated in schizophrenic patients (Austin et al. 2004; Ma et al. 2002; Morris et al. 2003). Other candidate genes are neuregulin 1 (Stefansson et al. 2002), a gene involved in various developmental steps, including migration of oligodendrocytes and myelin formation; dysbindin (Straub et al. 2002), a coiled-coil-containing protein binding to dystrobrevins and present at high expression levels in hippocampal mossy fiber terminals, G72 (Chumakov et al. 2002), associated with D-aminoacid oxydase and the regulator of G-protein signaling 4 (RGS4) (Mirnics et al. 2001). Etiologically relevant might also be the catechol-O-methyltransferase gene (Li et al. 1996) located in the velocardiofacial syndrome region on chromosome 22q11. The extracellular matrix glycoprotein reelin has also been implicated in schizophrenic symptoms, since it is down-regulated in schizophrenic patients (Tissir and Goffinet 2003). Finally, disease susceptibility has been recently associated with a genetic variation in the 8p21.3 gene, PPP3CC, encoding the calcineurin gamma subunit (Gerber et al. 2003).
Mice deficient in neuregulin 1 are available and have shown some schizophrenic symptoms, such as prepulse inhibition impairment (resistant to the atypical antipsychotic drug clozapine) and hyperactivity (clozapine-sensitive, Stefansson et al. 2002). Catechol-O-methyltransferase-deficient mice display increased anxiety and more aggressive behavior but no impairment of prepulse inhibition (Gogos et al. 1998).

Heterozygous reelin-deficient mice have a number of abnormalities resembling symptoms present in schizophrenia (Tissir and Goffinet 2003). However, complete absence of reelin causes severe brain malformation and the death of homozygous animals which bears little similarity to schizophrenia.

5.3   Potential value of the CHL1 deficient mouse

5.3.1 General evaluation

Several features of the CHL1 deficient mouse attract attention with regard to its usefulness in neuropsychiatric research. Structural aberrations are found in these animals, as shown by previous work (Montag-Sallaz et al. 2002) and in this study, indicating the usefulness with regard to the developmental etiology of schizophrenia. These aberrations are, importantly, not severe malformations but rather discrete abnormalities as are those observed in schizophrenic patients (Falkai et al. 2001). Among the structural defects observed in the CHL1 deficient mouse are defects in the connectivity of hippocampal and olfactory circuitries (Montag-Sallaz et al. 2002). Schizophrenia is most likely a disease of abnormal synaptic connectivities and functions (Frankle et al. 2003). And, as shown in this study, in the CHL1-/- mouse there is an abnormal postnatal dynamics in distinct cell populations which fits to the developmental delay in the natural history of the disease. Furthermore, a sensorimotor gating deficiency, assumed to be the pathophysiological basis of the human disease, is present in these animals as indicated by disrupted prepulse inhibition (Irintchev et al. 2004a). Moreover, the behavior of the animals is different from that of non-deficient littermates (Montag-Sallaz et al. 2002), as should be expected for a model of psychosis. There are deficiencies in the structure and function of inhibitory synapses in CHL1-/- animals (Nikonenko et al. 2004) and GABAergic transmission is apparently affected in patients (Reynolds et al. 2001; Lewis et al. 2004). And finally, there is evidence that the CALL (CHL1) gene in humans might be a susceptibility gene for schizophrenia (Sakurai et al. 2002, Chen et al. 2005). All these features make the CHL1 deficient mouse most attractive for neuropsychiatric research.

5.3.2 Similarities of structural aberrations in CHL1-/- mice and findings in schizophrenic patients

Over decades schizophrenia has been considered to be a "functional" psychosis mainly because neuropathologists failed to identify morphological alterations in the CNS of schizophrenic patients as reviewed in an article by Roberts and Bruton (1990) entitled "Notes from the graveyard: neuropathology and schizophrenia". Over the last years things have changed primarily due to the use of new non-invasive techniques such as computed tomography (CT) and structural magnetic resonance imaging (MRI), as well as to more systematic and sophisticated analyses of post-mortem brain samples from patients. Ventricular enlargement, dilatation of cortical sulci, gray matter reduction and dysplasia in the limbic system are the best documented morphological alterations in schizophrenics (Bogerts 1999).

5.3.2.1 Ventricles

Out of 47 well designed studies 79% find a lateral ventricular enlargement in schizophrenic patients (McCarley et al. 1999). The third ventricle has also been affected in more than 60% of the studies (McCarley et al. 1999). Ventricular dilatation has been proposed to be a good predictor of long-term therapeutic success and of disease outcome (Lieberman et al. 1992). The enlargement does not seem to be progressive in schizophrenic patients (Bogerts 1999). Although the exact cause of the changes in ventricular volume in schizophrenia remains unclear and ventriculomegalia is not specific for psychoses, this feature is the neuropathological hallmark of the disease. Ventricular enlargement is also present in the CHL1-/- mouse (Montag-Sallaz et al. 2002, 4.1.2). Our quantitative analysis showed a difference of about a factor of 2 between CHL1-/- and CHL1+/+ animals which appears to be large. Compared to the total brain volume (about 400 mm^3, see 4.1.1), however, the difference (about 4 mm^3, see 4.1.2) is small (< 1% of the total brain volume). In contrast, L1 deficient mice on the same C57BL/6J genetic background develop severe hydrocephalus (Rolf et al. 2001).

5.3.2.2 Motor Cortex and Cingulate Cortex

Along with the enlargement of ventricles, gray matter reduction, especially in the dorsolateral prefrontal and temporal cortex, is one of the most consistent findings in schizophrenic patients (Sullivan et al. 1998). Our analysis of the cortical thickness, however, did not reveal differences between mutant animals and wild-type littermates (see 4.1.3).

A variety of studies suggest that GABA interneurons in the cortex are prominently affected (Reynolds et al. 2001; Lewis et al. 2004). The GABAergic system has been implicated in the pathophysiology of schizophrenia for decades, especially with regard to its influence on the dopaminergic system. A lot of data argue for a defect in the GABAergic system of the frontal cortex: reduced amounts of mRNA and protein for the 67kDa isoform of glutamate decarboxylase (GAD_{67}), a GABA synthesizing enzyme (Akbarian et al. 1995; Volk et al. 2000) are paralleled by lower GABA concentrations (Kutay et al. 1989), less release of GABA (Sherman et al. 1991), lower levels of GAT1 mRNA (Volk et al. 2001) and up-regulation of $GABA_A$ sites (Dean et al. 1999).

GABAergic interneurons can be divided into several subgroups based on morphological characteristics and expression of different calcium binding proteins (Conde et al. 1994, Freund 2003). Chandelier neurons and wide basket neurons express parvalbumin whereas double bouquet neurons express calretinin (Lund and Lewis 1993). It can be presumed that chandelier neurons are the ones which might predominantly be involved in the pathophysiology of schizophrenia. The axon terminals of chandelier neurons form synapses exclusively with the axon initial segment of pyramidal neurons which is located very close to the site of action potential generation. Chandelier neurons therefore have a strong influence on the regulation of the excitatory output of pyramidal neurons playing a crucial role in working memory which is altered in schizophrenia. In addition, parvalbumin-containing neurons get input from dopaminergic axons and thalamocortical projections (Sesack et al. 1998), two systems projecting to the PFC, which is a structure essential for the working memory and apparently highly implicated in schizophrenia.

Last, but not least, does the density of parvalbumin-positive chandelier neurons change substantially during puberty, the age of onset of schizophrenia. A quantitative analysis of Brocca area 10 (PFC) revealed a decrease of parvalbumin-positive neurons in schizophrenic patients compared to normal controls.

Consequently, we used the maker parvalbumin in order to analyze the GABAergic system in two cortical areas. The analysis of the motor cortex revealed abnormally high numbers of PV+ cells in 2-month-old CHL1-/- animals compared to CHL1+/+ mice which declined to normal levels in older animals. Such an age-related decline was not detected in the cingulate cortex. These findings bear similarities with schizophrenia in two respects: in the first place, the alterations are region-specific, and, secondly, age-related.

Reelin is a glycoprotein which is produced by Cajal-Retzius cells and secreted into the ECM (D`Arcangelo et al. 1995). It plays a crucial role in neuronal migration, neuronal positioning and cerebral cortex lamination. Reelin is also involved in plasticity in the adult brain. The reeler mutant in mice (Reelin deficient mouse) does not show a normal pattern of cell migration throughout the cerebral and cerebellar cortices. The "inside-out" arrangement seen in wild-type mice is inverted to an "outside-in" pattern in the reeler mouse. Reelin expression has been found to be down-regulated in the PFC, temporal cortex, hippocampus, caudate nucleus, and cerebellum of schizophrenic patient`s brains (Benes et al. 1996a). Our findings in the motor cortex correlate with the findings in patients: at all ages the numbers of reelin+ interneurons were significantly lower in CHL1-/- animals as compared to CHL1+/+ littermates (see Table 3and 4.3.5). And here again region-specific differences were found. In comparison to the motor cortex, there was no reduction of reelin+ cells in the cingulate cortex in mutant animals. Rather there was a tendency for higher numbers at all three ages studied (Table 3 and 4.4.)

The increased density of Iba1 positive cells at 2 months of age in the motor cortex of mutant animals deserves also attention with respect to findings in patients with schizophrenia. In some cases, increased numbers of microglial cells have been observed (Bayer et al. 1999a; Radewicz et al. 2000), similar to the motor cortex of the CHL1-/- mouse at a young age (see 4.3.7) Mostly, however, microgliosis is not observed and this was the finding in the CHL1 mutant mouse at older ages. Therefore, an increase in the number of microglial cells may commonly occur in specific brain regions at younger ages of the patients but the phenomenon has not been encountered since typically older patients are studied.

5.3.2.3 Hippocampus

The hippocampus is part of the limbic system which is essential, among other functions, for the suppression of irrelevant information that reach the cortex along the afferent pathways. The hippocampus is essential for comparing past and present incoming sensory data and evaluating these data for emotional relevance (Mesulam 1986). Most of the studies regarding the limbic system of schizophrenic patients show subtle structural defects such as volume loss, cell loss and cytoarchitectural abnormalities but the type and extend of the limbic system pathology in schizophrenia varies (Harrison 2004). In contrast to degenerative diseases, limbic tissue volumes, cell numbers and size differ by some 10-20% between schizophrenics and controls including a considerable overlap between patients and controls. Structural and functional disturbances in the limbic system may lead to a dissociation of higher cognitive processes from elementary emotional models of response (Bogerts 1999).

Montag-Sallaz et al. (2002) studied the structure of the hippocampus in CHL1 deficient mice and found an altered configuration of the mossy fiber tract. The strict organization of the projections into two distinct bundles, a suprapyramidal and a infrapyramidal one, is lost in the CHL1 mutant mouse and fibers project through the CA3 pyramidal layer forming a network between the bundles. In this study, another subtle abnormality, a larger cross-sectional area of the pyramidal cell layer in CHL1-/- compared to CHL1+/+ animals, was found (see 4.1.4). The difference was present but small at all ages studied (about 10%). A similar difference in the volume of the CA1 pyramidal cell layer has recently been observed in one-month-old CHL1 deficient animals compared to wild-type control animals (Nikonenko et al. 2004). And, importantly, in that study the number of pyramidal cells in the mutant animals was found to be increased proportionally to the increase in size of the structure. Therefore, it can be concluded that the CHL1 deficiency leads to a discrete abnormality in the development of the pyramidal cell layer of the hippocampus. The increase in the volume of the pyramidal layer might appear too small to be of any substantial significance at first glance. The physiological consequences however are unpredictable, especially with regard to the possibility that this aberration could be accompanied or related to other abnormalities such as abnormalities in the dendritic trees of the pyramidal cells.

In the hippocampus of the CHL1 deficient mouse we also observed an age-related decline in the number of PV+ interneurons correlating with a transient

microgliosis. In schizophrenia, there is also evidence for deficits in GABA uptake (Reynolds et al. 1990) with increased (possibly compensatory) $GABA_A$ receptor binding (Benes et al. 1996a).

5.3.2.4 Substantia nigra and ventral tegmental area

A hypodopaminergic state of mesocortical dopamine transmission paralleled by a hyperdopaminergic state of mesolimbic dopamine transmission has been suggested to be relevant to the pathophysiology of schizophrenia (Ballmaier et al. 2002). Therefore, we analyzed the dopaminergic system. The ventral tegmental area (VTA) is the neuronal source of the mesolimbic dopaminergic pathway and has been proposed to be related to psychotic symptoms and information processing dysfunction in schizophrenia (O´Donell and Grace 1998). A hyperactivity of mesolimbic dopaminergic neurons is suggested to produce the positive symptoms of schizophrenia (Seeman 1987) and a hypodopaminergic state of mesocortical dopaminergic neurons is proposed to be the basis of negative symptoms (Dworkin and Opler 1992).

Regarding the proposed pathophysiological relevance of the mesotelencephalic dopaminergic system in schizophrenia and its possible link with cortical alterations, we investigated whether there is evidence that the nigro-striatal dopaminergic system is altered in CHL1 deficient mice by evaluating the numerical density of tyrosine hydroxylase positive cells in the substantia nigra. We found no difference between the genotypes at two months of age but a significant reduction in the number of TH positive neurons in the substantia nigra of older CHL1 deficient mice (see 4.6). This suggests that TH+ neurons are lost with age in the mutant animals which would certainly have an impact on the behavior of these animals. Numbers of dopaminergic cells have yet not been estimated in samples from patients.

5.3.2.5 Age dependency

We know that first signs of the disease process are already present in young children who will later on develop schizophrenia but the disease specific symptoms only evolve after puberty. Therefore pathological changes in the patient´s brains must occur between childhood and adulthood. In our study we could show age-dependent alterations of gross anatomical parameters and numerical densities of

immunohistochemically identified cell populations in CHL1 deficient mice. Mice at 2, 6 and 12 months of age were studied, ages that can be compared to young adulthood, adulthood and old age in humans, respectively. Our data suggest that dynamic processes occur between young adulthood, adulthood and old age in CHL1-/- mice a finding consistent with the clinical time course of schizophrenia.

5.4 Conclusion

The present study has identified structural aberrations in the CHL1 deficient mouse which are strongly reminiscent of abnormalities that have been identified in brains of patients with schizophrenia. Moreover, the investigation of animals at different ages revealed a striking postnatal dynamics. This dynamics correlates with the developmental delay in the clinical manifestation of the human disease. These features, in conjunction with other known behavioral and physiological abnormalities, make the CHL1 mutant mouse a most promising model for future neuropsychiatric research. Ultimately an animal model of schizophrenia may help to expand our knowledge of this poorly understood disorder, which strikes at the very core of what it means to be human. A better understanding of the disease would give us new therapeutic approaches which will deal with the actual cause of the disease (a defective protein synthesis for example) instead of dealing with the consequences (dysfunction in the dopaminergic system) as we do today. Having found the potential genetic cause ("first hit") of the disease we will continue to search for a "second hit" using CHL1 deficient mice. Inducing maternal viral infections or anoxia during birth will be one way of approaching this target. Finally knowing the first and second hit which give rise to the disease a screening test could be developed helping to prevent a second hit in already susceptible individuals carrying a genetic muation like CHL1.

6 SUMMARY

Schizophrenia is one of the most devastating diseases striking mankind at the high frequency of about 1%. Its etiology is poorly understood and it is generally believed that animal models resembling the disease in particular features might be helpful. Although several models have been proposed, their suitability is restricted. More promising might be a newly generated mouse deficient in the expression of the cell adhesion molecule <u>c</u>lose <u>h</u>omologue of <u>L1</u> (CHL1). CHL1 belongs to the immunoglobulin superfamily of cell adhesion molecules. It is implicated in neuronal migration, neurite outgrowth and fasciculation, synapse formation and plasticity. Existing evidence indicates that mutations in the gene encoding CHL1 may cause brain malformations and dysfunctions in both humans and mice. Furthermore, genetic linkage studies have identified the CHL1 gene as a putative susceptibility factor for schizophrenia and prepulse inhibition (PPI) of acoustic startle has been found to be disrupted in CHL1 mutant mice which is a measure of the ability to gate the flow of sensorimotor information, and disturbances characterize major psychiatric disorders including schizophrenia.

This study was designed to further characterize the CHL1 mutant mouse with respect to morphological abnormalities in the brain structures known to be affected in schizophrenic patients. Morphometric as well as stereological analyses of immunohistochemically identified major cell types (neurons, neuronal subpopulations, astrocytes, oligodendrocytes and microglia) were performed. Areas studied included the motor and cingulate cortex, the cerebral ventricles, the hippocampus and the substantia nigra. CHL1 deficient (CHL1-/-) and non-deficient (CHL1+/+) mice at 2, 6 and 12 months of age were investigated, ages that can be compared to adolescence, and early and mid-adulthood in humans, respectively.

Abnormal features identified in CHL1-/- animals at all ages studied were ventriculomegalia (enlarged ventricles) and hippocampal dysplasia with respect to the size of the CA region (enlarged as compared to control animals). The motor cortex of the mutant animals was deficient in reelin-expressing inhibitory neurons at all ages. More interestingly, consistent with the maturational delay thought to be a feature of schizophrenia, an age-related decline of PV+ cell density in the hippocampus and motor cortex was found to occur between 2 and 6 months of age without changes in hippocampal cross-sectional area and cortical thickness. A similar reduction was seen

for the total cell density in the motor cortex and dopaminergic cells in the substantia nigra. Surprisingly, also a small but significant age-related increase in brain mass was found in the CHL1-/- mice. In contrast to the hippocampus and motor cortex, no significant differences were observed in the cingulate cortex for any parameter studied indicating that CHL1 deficiency differentially affects specific brain regions. Finally, densities of microglial cells (Iba1$^+$), commonly related to neurodegenerative processes, were increased in the also otherwise affected regions at two months of age in the CHL1-/- animals and these differences disappeared at older ages.

In conclusion, the CHL1 mutation, in addition to causing gross structural abnormalities, affects inhibitory interneurons and the dopaminergic system in a region-specific and age-related way that strikingly correlates with abnormalities observed in schizophrenic patients. This evidence identifies the CHL1 deficient mouse as a new valuable model for neuropsychiatric research.

7 REFERENCES

Akbarian S, Kim JJ, Potkin SG, Hagman JO, Tafazzoli A, Bunney Jr WE, Jones EG (1995) Gene expression for glutamic acid decarboxylase is reduced without loss of neurons in prefrontal cortex of schizophrenics. Arch Gen Psychiatry 52: 258-266

Andersen SL (2003) Trajectories of brain development: point of vulnerability or window of opportunity? Neuroscience and Biobehavioral Reviews 27: 3-18

Asai M, Ito Y, Iguchi T, Ito J, Okada N, Oishi H (1992) Terminal deletion of the short arm of chromosome 3. Jpn J Hum Genet 37: 163-168

Austin CP, Ky B, Ma L, Morris JA, Shughrue PJ (2004) Expression of disrupted-in-schizophrenia-1, a schizophrenia-associated gene, is prominent in the mouse hippocampus throughout brain development. Neuroscience 124: 3-10

Ballmaier M, Zoli M, Leo G, Agnati LF, Spano PF (2002) Preferential alterations in the mesolimbic dopamine pathway of heterozygous reeler mice: an emerging animal-based model of schizophrenia. European Journal of Neuroscience 15: 1197

Barbeau D, Liang JJ, Robitalille Y, Quirion R, Srivastava LK (1995) Decreased expression of the embryonic form of the neural cell adhesion molecule in schizophrenic brains. Proc Natl Acad Sci USA 92: 2785-2789

Basset AS (1991) Linkage analysis of schizophrenia: challenges and promise. Soc Biol 38: 189-196

Bayer TA, Buslei R, Havas L, Falkai P (1999a) Evidence for activation of microglia in patients with psychiatric illnesses. Neurosci Lett 271: 126-128

Bayer TA, Falkei P, Meier W (1999b) Genetic and non-genetic vulnerability factors in schizophrenia: the basis of the "two hit hypothesis". J Psychiatr Res 33: 543-548

Benes FM, Khan Y, Vincent SL, Wickramasinghe R (1996a) Differences in the subregional and cellular distribution of $GABA_A$ receptor binding in the hippocampal formation of schizophrenic brain. Synapse 22: 338-349

Berger N, Vaillancourt C, Boska P (2000) Genetic factors modulate effects of C-section birth on dopaminergic function in the rat. Neuroreport 11: 639-643

Bixby JL, Lilien J, Reichardt LF (1988) Identification of the major proteins that promote neuronal process outgrowth on Schwann cells in vitro. J. Cell Biol. 107: 353-362

Black DW, Andreasen NC (1999) Schizophrenia, Schizophreniform and Delusional (Paranoid) Disorders. In: The American Psychiatric Association Textbook of Psychiatry, Washington, pp: 425-478

Bogerts B (1999) The neuropathology of schizophrenic diseases: historical aspects and present knowledge. Eur Arch Psychiatry Clin Neurosci 249: 2-13

Boska P, Wilson D, Rochford J (1998) Responses to stress and novelty in adult rats born vaginally, by cesarean section or by cesarean section with acute anoxia. Biol Neonate 74: 48-59

Brackenbury R, Thiery JP, Rutishauser U, Edelman GM (1977) Adhesion among neural cells of the chick embryo. I. An immunological assay for molecules involved in cell-cell binding. J Biol Chem 252: 6835-6840

Braff DL, Geyer MA and Swerdlow NR (2001) Human studies of prepulse inhibition of startle: normal subjects, patient groups, and pharmacological studies. Psychopharmacology 156: 234-258

Braun AR, Jaskiw GE, Vladar K, Sexton RH, Kolachana BS, Weinberger DR (1993) Effects of ibotenic acid lesion on the medial prefronatal cortex on dopamine agonist related behaviours in the rat. Pharmacol Biochem Behav 46: 51-60

Chaisuksunt V, Campbell G, Zhang Y, Schachner M, Lieberman AR, Anderson PN (2000a) The cell recognition molecule CHL1 is strongly upregulated by injured and regenerating thalamic neurons. J Comp Neurol 425: 382-392

Chaisuksunt V, Zhang Y, Anderson PN, Campbell G, Vaudano E, Schachner M, Lieberman AR (2000b) Axonal regeneration from CNS neurons in the cerebellum and brainstem of adult rats: Correlation with the patterns of expression and distribution of messenger RNAs for L1, CHL1, c-jun and growth associated protein 43. Neuroscience 100: 87-108

Chen QY, Chen Y, Feng GY, Lindpainter K, Chen Y, Sun X, Chen Z, Gao Z, Tang J, He L (2005) Case-control association study of close homologue of L1 (CHL1) and schizophrenia in the Chinese population. Schizophr Res. 73: 269-274

Chen S, Mantei L, Dong L, Schachner M (1999) Prevention of neuronal cell death by neural adhesion molecules L1 and CHL1. J Neurobiol 38: 428-439

Chumakov I, Blumenfeld M, Guerassimenko O, Cavarec L, Palicio M, Abderrahim H, Bougueleret L, Barry C, Tanaka H, La Rosa P, Puech A, Tahri N, Cohen-Akenine A, Delabrosse S, Lissarrague S, Picard FP, Maurice K, Essioux L, Millasseau P, Grel P, Debailleul V, Simon A, Caterina D, Dufaure I, Malekzadeh K, Belova M, Luan J, Bouillot M, Sambucy JL, Primas G, Saumier M, Boubkiri N, Martin-Saumier S, Nasroune M, Peixoto H, Delaye A, Pinchot V, Bastucci M, Guillou S, Chevillon M, Sainz-Fuertes R, Meguenni S, Aurich-Costa J, Cherif D, Gimalac A, Van Duijn C, Gauvreau D, Ouellette G, Fortier I, Raelson J, Sherbatich T, Riazanskaia N, Rogaev E, Raeymaekers P, Aerssens J, Konings F, Luyten W, Macciardi F, Sham PC, Straub RE, Weinberger DR, Cohen N, Cohen D (2002) Genetic and physiological data implicating the new human gene G27 and the gene for D-amino acid oxidase in schizophrenia. Proc Natl Acad Sci: 13365-13367

Cloninger CR (1997) Multilocus genetics of schizophrenia. Curr Opin Psych 10: 5-10

Cohen NR, Taylor JSH, Scott LB, Guillery RW, Soriano P, Furley AJW (1997) Errors in corticospinal axon guidance in mice lacking the neural cell adhesion molecule L1. Curr Biol 7: 26-33

Cole GJ, Burg M (1989) Characterization of a heparan sulfate proteoglycan copurifies with the cell adhesion molecule. Exp. Cell Res 182: 44-60

Collinson JM, Marshall D, Gillespie CS, Brophy PJ (1998) Transient expression of neurofascin by oligodendrocytes at the onset of myelinogenesis: implications of mechanisms of axon-glial interactions. Glia 23: 11-23

Conde F, Lund JS, Jacobowitz DM, Baimbridge KG, Lewis DA (1994) Local circuit neurons immunoreactive for calretinin, calbindin D28k or parvalbumin in monkey prefrontal cortex: distribution and morphology. Journal of Comparative Neurology 341: 95-116

Cowan WM, Harter DH, Kandel ER (2000) The emergence of modern neuroscience: some implications for neurology and psychiatry. Annu Rev Neurosci 23: 343-391

Cremer H, Lange R, Christoph A, Plomann M, Vopper G, Roes J, Brown R, Baldwin S, Barthels D, Rajewski K, Wille W (1994) Inactivation of the NCAM gene in mice results in size reduction of the olfactory bulb and deficits in spatial learning. Nature 367: 455-459

Cunningham BA, Hemperly JJ, Murray BA, Prediger EA, Brackenbury R, Edelman GM (1987) Neural cell adhesion molecule: structure, immunoglobulin-like domains, cell surface modulation and alternative RNA splicing. Science 236: 799-806

Cunningham BA (1995) Cell adhesion molecules as morphoregulators. Curr Opin Cell Biol 7: 628-633

Dahme M, Bartsch U, Martini R, Anliker B, Schachner M, Mantei N (1997) Disruption of the mouse L1 gene leads to malformations of the nervous system. Nat Genet 17: 346-349

D`Arcangelo G, Miao GG, Chen SC, Soares HD, Morgan JI, Curran T (1995) A protein related to extracellular matrix proteins deleted in the mouse mutant reeler. Nature 374: 719-723

Dean B, Hussain T, Hayes W, Scarr E, Kitsoulis S, Hill C, Opeskin K, Copolov DL (1999) Changes in serotonin$_{2A}$ and and GABA$_A$ receptors in schizophrenia, studies on the human dorsolateral prefrontal cortex. Journal of Neurochemistry 72: 1593-1599

Demyanenko GP, Anton E, Schachner M, Feng G, Sanes J, Maness PF (2004) Close homolog of L1 modulates area-specific neuronal positioning and dendrite orientation in the cerebral cortex. Neuron 44: 423-437

Drumheller T, Mc Gillivray BC, Behrner D, MacLeod P, Mc Fadden DE, Roberson J, Venditti C, Chorney M, Smith DI (1996) Precise localisation of 3p25 breakpoints in four patients with the 3p-syndrome. J Med Genet 33: 842-847

Dworkin RH, Opler LA (1992) Simple schizophrenia, negative symptoms, and prefrontal hypodopaminergia. Am J Psychiatry 149: 1284-1285

El Khodor BF, Boska P (1998) Birth insult increases amphetamine-induced behavioral responses in the adult rat. Neuroscience 87: 893-904

Falkai P, Vogeley K, Maier W (2001) Hirnstrukturelle Veränderungen bei Patienten mit schizophrenen Psychosen. Nervenarzt 72: 331-341

Feinberg I (1982) Schizophrenia: caused by a fault in programmed synaptic elimination during adolescence? J Psychiatr Res 17: 319-334

Fischer G, Künemund V, Schachner M (1986) Neurite outgrowth patterns in cerebellar microexplant cultures are affected by antibodies to the cell surface glycoprotein L1. J Neurosci 6: 605-612

Frankle WG, Lerma J, Laurelle M (2003) The synaptic hypothesis of schizophrenia. Neuron 39: 205-216

Franklin KBJ, Paxinos G (1997) The mouse brain in stereotaxic coordinates. Academic Press, San Diego

Fransen E, Lemmon V, Van Camp G, Vits L, Coucke P, Willems PJ (1995) CRASH syndrome: Clinical spectrum of corpus callosum hypoplasia, retardation, adducted thumbs, spastic paraparesis and hydrocephalus due to mutations in one single gene, L1. Eur. J. Hum. Genet. 3: 273-284

Fransen E, DiHooge R, Camp GV, Verhoye M, Sijbers J, Reyniers E, Soriano P, Kamiguchi H, Willemsen R, Koekkoek SKE, De Zeeuw CI, De Deyn PP, Van der Linden A, Lemmon V, Kooy RF, Willems PJ (1998) L1 knockout mice show dilated ventricles, vermis hypoplasia and impaired exploration patterns. Hum Mol Genet. 7: 999-1009

Freund TF (2003) Interneuron diversity series: rhythm and mood in perisomatic inhibition. Trends Neurosci 26: 489-495

Friedlander DR, Milev P, Karthikeyan L, Margolis RK, Margolis RU, Grumet M (1994) The neuronal chondroitin sulfate proteoglycan neurocan binds to the neural cell adhesion molecules Ng-CAM/ L1/ NILE and NCAM, and inhibits neuronal adhesion and neurite outgrowth. J Cell Biol 125: 669-680

Frints SG, Marynen P, Hartmann D, Fryns JP, Steyaert J, Schachner M, Rolf B, Craessaerts K, Snellinx A, Hollanders K, D'Hooge R, De Deyn PP, Froyen G (2003) CALL interrupted in a patient with non-specific mental retardation: gene dosage-dependent alteration of murine brain development and behavior. Hum. Mol. Genet. 12: 1463-1474

Fukuda T, Kosaka T (2000) The dual network of GABAergic interneurons linked by both chemical and electrical synapses: a possible infrastructure of the cerebral cortex. Neurosci Res 38: 123-130

Galarreta M, Hestrin S (2002) Electrical and chemical synapses among parvalbumin fast-spiking GABAergic interneurons in adult mouse neocortex. Proc Natl Acad Sci 99: 12438-12443

Geddes JR, Lawrie SM (1995) Obstetric complications and schizophrenia: a meta analysis. Br J Psychiatry 167: 786-793

Geisler S, Heilmann H, Veh RW (2002) An optimized method for simultaneous demonstration of neurons and myelinated fiber tracts for delineation of individual trunco-and palliothalamic nuclei in the mammalian brain. Histochem Cell Biol, 117: 69-79

Gerber DJ, Hall D, Miyakawa T, Demars S, Gogos JA, Karayiorgou M, Tonegawa S (2003) Evidence for association of schizophrenia with genetic variation in the 8p21.3 gene, PPP3CC, encoding the calcineurin gamma subunit. Proc. Natl. Acad. Sci. U.S.A 100: 8993-8998

Gogos JA, Morgan M, Luine V, Santha M, Ogawa S, Pfaff D, Karayiorgou M (1998) Catechol-O-methyltransferase-deficient mice exhibit sexually dimorphic changes in catecholamine levels and behavior. Proc Natl Acad Sci U.S.A 95: 9991-9996

Gottesman I.I (1991) Schizophrenia Genesis: The Origins of Madness. W.H. Freeman, New York

Grumet M, Sakurai T (1996) Heterophilic interactions of the neural cell adhesion molecules Ng-CAM and Nr-CAM with neural receptors and extracellular matrix proteins. Seminars Neurosci 8: 379-389

Harding BN (1992) Malformations of the nervous system. In: Adams JH, Duchen LW, editors. Greenfield´s neuropathology, 5th ed. London p. 521-638

Harrison PJ (2004) The hippocampus in schizophrenia: a review of the neuropathological evidence and its pathophysiological implications. Psychopahrmacology 174: 151-162

Harrison PJ, Owen MJ (2003) Genes for schizophrenia? Recent findings and their pathophysiological implications. Lancet 361: 417-419

Hillenbrand R, Molthagen M, Montag D, Schachner M (1999) The close homologue of neural adhesion molecule L1 (CHL1): patterns of expression and promotion of neurite outgrowth by heterophilic interactions. Eur J Neurosci 11: 813-826

Hoffman S, Edelman GM (1983) Kinetics of homophilic binding by embryonic and adult forms of the neural cell adhesion molecule. Proc Natl Acad Sci USA 80: 5762-5766

Holm J, Hillenbrand R, Steuber V, Bartsch U, Moos M, Lübbert H, Montag D, Schachner M (1996) Structural features of a close homologue of L1 (CHL1) in the mouse: a new member of the L1 family of neural recogntion molecules. Eur J Neurosci 8: 1613-1629

Imai Y, Kohsaka S (2002) Intracellular signaling in M-CSF-induced microglia activation: role of Iba1. Glia 40: 164-174

Irintchev A, Rollenhagen A, Tronscoso E, Kiss JZ, Schachner M (2004a) Structural and functional aberrations in the cerebral cortex of tenascin-C deficient mice. Cereb Cortex Nov10 (Epub ahead of print)

Irintchev A, Koch M, Needham LK, Maness P and Schachner M (2004b) Impairment of sensorimotor gating in mice deficient in the cell adhesion molecule L1 or its close homologue, CHL1. Brain Res 1029: 131-134

Jaskiw GE, Karoum FK, Weinberger DR (1990) Persistent elevations in dopamine and its metabolites in the nucleus accumbens after mild subchronic stress in rats with ibotenic acid lesions of the medial prefrontal cortex. Brain Res 534: 321-323

Karayiorgou M, Gogos JA (1997) Dissecting the genetic complexity of schizophrenia. Mol Psychiatry 2: 211-223

Kendler KS, Diehl SR (1993) The genetics of schizophrenia: A current genetic-epidemiologic perspective. Schizophr. Bull 19: 261-285

Kilts CD (2001) The changing roles and targets for animal models of schizophrenia. Biol Psychiatry 50: 845-855

Knable MB (1999) Schizophrenia and bipolar disorder: findings from studies of the Stanley Foundation Brain Collection. Schizophr Res 39: 149-152

Kokkinidis L, Anisman H (1980) Amphetamine models of paranoid schizophrenia: an overview and elaboration of animal experimentation. Psychol Bull 88: 551-579

Kutay FZ, Pögün S, Hariri NI, Peker G, Erlacin S (1989) Free amino acid level determinations in normal and schizophrenic brain. Progress in Neuro-Psychopharmacology and Biological Psychiatry 13: 119-126

Lagenaur C, Lemmon V (1987) An L1-like molecule, the 8D9 antigen, is a potent substrate for neurite extension. Proc Natl Acad Sci USA 84: 7753-7757

Lewis G, David A, Andreasson S, Allebeck P (1992) Schizophrenia and city life. Lancet 340: 137-140

Lewis CM, Levinson DF, Wise LH, Delisi LE, Straub RE, Hovatta I, Williams NM, Schwab SG, Pulver AE, Faraone SV, Brzustowicz LM, Kaufmann CA, Garver DL, Gurling HMD, Lindholm E, Coon H, Moises HW, Byerley W, Shaw SH, Mesen A, Sherrington R, O'Neill FA, Walsh D, Kendler KS, Ekelund J, Paunio T, Lonnqvist J, Peltonen L, O'Donovan MC, Owen MJ, Wildenauer DB, Maier W, Nestadt G, Blouin JL, Antonarakis SE, Mowry BJ, Silverman JM, Crowe RR, Cloninger CR, Tsuang MT, Malaspina D, Harkavy-Friedman JM, Svrakic DM, Bassett AS, Holcomb J, Kalsi G, McQuillin A, Brynjolfson J, Sigmundsson T, Petursson H, Jazin E, Zoega T, Helgason T (2003) Genome scan meta-analysis of schizophrenia and bipolar disorder, part II: Schizophrenia. Am J Hum Genet. 73: 34-48

Lewis DA, Levitt P (2002) Schizophrenia as a disorder of neurodevelopment. Annu. Rev. Neurosci. 25: 409-432

Lewis DA, Volk DW, Hashimoto T (2004) Selective alterations in prefrontal cortical GABA neurotransmission in schizophrenia: a novel target for the treatment of working memory dysfunction. Psychopharmacology 174: 143-150

Li T, Sham PC, Vallada H, Xie T, Tang X, Murray RM, Liu X, Collier DA (1996) Preferential transmission of the high activity allele of COMT in schizophrenia. Psychiatr Genet. 6: 131-133

Lieberman J, Bogerts B, Degreef G, Ashtari M, Alvir J (1992) Qualitative assessment of brain morphology in acute and chronic schizophrenia. Am J Psychiatry 149: 784-791

Lipska BK, Jaskiw GE, Weinberger DR (1993) Postpubertal emergence of hyperresponsiveness to stress and to amphetamine after neonatal excitotoxic hippocampal damage: a potential animal model of schizophrenia. Neuropsychopharmacology 9: 67-75

Lipska BK, Weinberger DR (1993) Delayed effects of neonatal hippocampal damage on haloperidol-induced catalepsy and apomorphine induced stereotypic behaviours in the rat. Brain Res Dev Brain Res 75: 213-222

Lund JS, Lewis DA (1993) Local circuit neurons of developing and mature macaque prefrontal cortex, Golgi and immunocytochemical characteristics. Journal of Comparative Neurology 328: 282-312

Luthl A, Laurent JP, Figurov A, Muller D, Schachner M (1994) Hippocampal long-term potentiation and neural cell adhesion molecules L1 and NCAM. Nature 372: 777-779

Ma L, Liu Y, Ky B, Shughrue PJ, Austin CP, Morris JA (2002) Cloning and characterization of Disc1, the mouse ortholog of DISC1 (Disrupted-in-Schizophrenia 1). Genomics 80: 662-672

Marcotte ER, Pearson DM, Srivastava LK (2001) Animal models of schizophrenia: a critical review. Psychiatry Neurosci 26: 395-410

Marder SR (1999) Limitations of Dopamine-D2 Antagonists and the Search for Novel Antipsychotic Strategies. Neuropsychopharmacology 21: 117-121

McCarley RW, Wible CG, Frumin M, Hirayasu Y, Levitt JJ, Fischer IA, Shenton ME (1999) MRI anatomy of schizophrenia. Biol Psychiatry 45: 1099-1119

McGrath JJ, Feron FP, Burne TH, Mackay-Sim A, Eyles DW (2003) The neurodevelopmental hypothesis of schizophrenia: a review of recent developments. Ann. Med. 35: 86-93

Mc Neil TF, Cantor-Graae E, Blenow G (1996) Do clumsy fetuses cause labor and delivery complications?: A study of offspring at risk for psychosis. Schizophr Res 22: 85-88

Mesulam MM (1986) Patterns in behavioral neuroanatomy: association areas, the limbic system, and hemispheric specialization. In: Mesualem MM (ed) Principles of behavioral neurology. Davis, Philadelphia, pp 1-70

Mirnics K, Middleton FA, Stanwood GD, Lewis DA, Levitt P (2001) Disease-specific changes in regulator of G-protein signaling 4 (RGS4) expression in schizophrenia. Mol Psychiatry 6: 293-301

Montag-Sallaz M, Schachner M, Montag D (2002) Misguided axonal projections, neural cell adhesion molecule 180 mRNA upregulation and altered behavior in mice deficient for the close homologue of L1. Molecular and cellular Biology: 7967-7981

Montgomery AM, Becker JC, Siu CH, Lemmon VP, Cheresh DA, Pancook JD, Zhao X, Reisfeld RA (1996) Human neural cell adhesion molecule L1 and rat homologue NILE are ligands for integrin alpha v beta 3. J Cell Biol 132: 475-485

Moran LB, Graeber MB (2004) The facial nerve axotomy model. Brain Res Rev 44: 154–178

Morris JA, Kandpal G, Ma L, Austin CP (2003) DISC1 (Disrupted-In-Schizophrenia 1) is a centrosome-associated protein that interacts with MAP1A, MIPT3, ATF4/5 and NUDEL: regulation and loss of interaction with mutation. Hum Mol Genet 12: 1591-1608

Myhrman A, Rantakallio P, Isohanni M, Jones P, Partanen U (1996) Unwantedness of a pregnancy and schizophrenia in the child. Br J Psychiatry 169: 637-640

Niemi LT, Suvisaari JM, Tuulio-Henriksson A, Lönnqvist JK (2003) Childhood developmental abnormalities in schizophrenia: evidence from high-risk studies. Schizophrenia Research 60: 239-258

O´Donell P, Grace AA (1998) Dysfunctions in multiple interrelated systems as the neurobiological bases of schizophrenic symptom clusters. Schizophr.Bull 24: 267-283

Owens GC, Edelman GM, Cunningham BA (1987) Organization of the NCAM gene-alternative exon usage as the basis for different membrane associated domains. Proc Natl Acad Sci USA 84: 294-298

Pesold C, Liu WS, Guidotti A, Costa E, Caruncho HJ (1999) Cortical bitufted, horizontal, and Martinotti cells preferentially express and secrete reelin into perineuronal nets, nonsynaptically modulating gene expression. Proc Natl Acad Sci USA 96: 3217-3222

Poltorak M, Khoja I, Hemperly JJ, Williams JR, EL-Mallakh R, Freed WJ (1995) Disturbances in cell recognition molecules (NCAM and L1 antigen) in the CSF of patients with schizophrenia. Exp Neurol 131: 266-272

Powers RE (1999) The neuropathology of schizophrenia. J Neuropathol Exp Neurol 58:679-690

Radewicz K, Garey LJ, Gentleman SM, Reynolds R (2000) Increase in HLA-DR immunoreactive microglia in frontal and temporal cortex of chronic schizophrenics. J Neuropathol Exp Neurol 59: 137-150

Reed MG, Howard CV (1998) Surface weighted star volume: concept and estimation. J Microsc 190: 350-356

Reynolds GP, Czudek C, Andrews HB (1990) Deficit and hemispheric asymmetry of GABA uptake sites in the hippocampus in schizophrenia. Biological psychiatry 27: 1038-1044

Reynolds GP, Zhang ZJ, Beasley CL (2001) Neurochemical correlates of cortical GABAergic deficits in schizophrenia: selective losses of calcium binding protein immunoreactivity. Brain Res Bull 55: 579-584

Roberts GW, Bruton CJ (1990) Notes from the graveyard: neuropathology and schizophrenia. Neuropathol Appl Neurobiol 16: 3-16

Rolf B, Kutsche M, Bartsch U (2001) Severe hydrocephalus in L1-deficient mice. Brain Res. 891: 247-251

Rutishauser U, Landmesser L (1996) Polysialic acid in the vertebrate nervous system: A promoter of plasticity in cell-cell interactions. Trends Neurosci 19: 422-427

Sakurai K, Migita O, Toru M, Arinami T (2002) An association between a missense polymorphism in the close homologue of L1 (CHL1, CALL) gene and schizophrenia. Mol Psych 7: 412-415

Scholey AB, Mileusnic R, Schachner M, Rose SP (1995) A role for a chicken homolog of the neural cell adhesion molecule L1 in consolidation of memory of a passive avoidance task in the chick. Learn Mem 2: 17-25

Seeman P (1987) Dopamine receptors and the dopamine hypothesis of schizophrenia. Synapse 1: 133-152

Seki T, Rutishauser U (1998) Removal of polysialic acid neural cell adhesion molecule induces aberrant mossy fiber inervation and ectopic synaptogenesis in the hippocampus. J Neurosci 18: 3757-3766

Sesack SR, Hawrylak VA, Melchitzky DS, Lewis DA (1998) Dopamine innervation of a subclass of local circuit neurons in monkey prefrontal cortex: Ultrastructural analysis of tyrosine hydroxylase and parvalbumin immunoreactive structures. Cereb Cortex 8: 614-622

Sherman AD, Davidson AT, Baruah S, Hegwood TS, Waziri R (1991) Evidence of glutamatergic deficiency in schizophrenia. Neuroscience Letters 121: 77-80

Sidman RL, Angevine JB and Peirce ET (1971) Atlas of the mouse brain and spinal cord. Harvard University Press, Cambridge, Massachusetts

Sofroniew MV and Schrell U (1982) Long-term storage and regular repeated use of diluted antisera in glass staining jars for increased sensitivity, reproducibility, and convenience of single-and two-color light microscopic immunocytochemistry. J Histochem Cytochem 30: 504-511

Stefansson H, Sigurdsson E, Steinthorsdottir V, Bjornsdottir S, Sigmundsson T, Ghosh S, Brynjolfsson J, Gunnarsdottir S Ivarsson O, Chou TT, Hjaltason O, Birgisdottir B, Jonsson H, Gudnadottir VG, Gudmundsdottir E, Bjornsson A, Ingvarsson B, Ingason A, Sigfusson S, Hardardottir H, Harvey RP, Lai D, Zhou M, Brunner D, Mutel V, Gonzalo A, Lemke G, Sainz J, Johannesson G, Andresson T, Gudbjartsson D, Manolescu A, Frigge ML, Gurney ME, Kong A, Gulcher JR, Petursson H, Stefansson K (2002) Neuregulin 1 and susceptibility to schizophrenia. Am J Hum Genet 71: 877-892

Storck O, Welzl H, Cremer H, Schachner M (1997) Increased intermale agression and neuroendocrine response in mice deficient for the neural cell adhesion molecules. Eur J Neurosci 9: 424-434

Straub RE, Jiang Y, MacLean CJ, Ma Y, Webb BT, Myakishev MV, Harris-Kerr C, Wormley B, Sadek H, Kadambi B, Cesare AJ, Gibberman A, Wang X, O`Neill FA, Walsh D, Kendler KS (2002)

Genetic variation in the 6p22.3 gene DTNBP1, the human ortolog of the mouse dysbindin gene, is associated with schizophrenia. Am J Hum Genet. 71: 337-348

Streit WJ, Walter SA, Pennel NA (1999) Reactive microgliosis. Progr Neurobiol 57: 563-581

Sullivan EV, Lim KO, Mathalon D, Marsh L, Beal DM, Harris D, Hoff AL, Faustman WO, Pfefferbaum A (1998) A profile of cortical gray matter volume deficits characteristic of schizophrenia. Cerebral Cortex 8: 117-124

Susser E, Neugebauer R, Hoek HW, Brown AS, Lin S, Labovitz D, Gorman JM (1996) Schizophrenia after prenatal famine. Further evidence. Arch Gen Psychiatry 53: 25-31

Swerdlow NR, Mansbach RS, Geyer MA, Pulvirenti L, Koob GF, Braff DL (1990) Amphetamine disruption of prepulse inhibition of acoustic startle is reversed by depletion of mesolimbic dopamine. Psychopharmacology 100: 413-416

Swerdlow NR, Geyer MA and Braff DL (2001) Neural circuit regulation of prepulse inhibition of startle in the rat: current knowledge and future challenges. Psychopharmacology 156: 194-215

Tacke R, Moos M, Teplow DB, Fruh K, Scherer H, Bach A, Schachner M (1987) Identification of cDNA clones of the mouse neural cell adhesion molecule L1. Neurosci Lett 82: 89-94

Tissir F, Goffinet AM (2003) Reelin and brain development. Nat Rev Neurosci 4: 496-505

Tomasiewicz H, Ono K, Yee D, Thompson C, Goridis C, Rutishauser U, Magnuson T (1993) Genetic deletion of a neural cell adhesion molecule variant (NCAM-180) produces distinct defects in the central nervous system. Neuron 11: 1163-1174

Van den Buuse M, Garner B, Koch M (2003) Neurodevelopmental animal models of schizophrenia: effects on prepulse inhibition. Curr Mol Med 3: 459-471

van Os J, Selten JP (1998) Prenatal exposure to maternal stress and subsequent schizophrenia. The May 1940 invasion of The Netherlands. Br J Psychiatry 172: 324-326

Volk DW, Austin MC, Pierri JN, Sampson AR, Lewis DA (2000) Decreased GAD_{67} mRNA expression in a subset of prefrontal cortical GABA neurons in subjects with schizophrenia. Arch Gen Psychiatry 57: 237-245

Volk DW, Austin MC, Pierri JN, Sampson AR, Lewis DA (2001) GABA transporter-1 mRNA in the prefrontal cortex in schizophrenia, decreased expression in a subset of neurons. American Journal of Psychiatry 158: 256-265

Walker EF (1994) Developmentally moderated expressions of the neuropathology underlying schizophrenia. Schizophr Bull 20: 453-80

Walker E, Kestler L, Bollini A, Hochman KM (2004) Schizophrenia: etiology and course. Annu. Rev. Psychol. 55: 401-430

Weinberger DR (1987) Implications of normal brain development for the pathogenesis of schizophrenia. Arch Gen Psychiatry 44: 660-669

Weller S, Gärtner J (2001) Genetic and clinical aspects of X-linked hydrocephalus (L1 disease): Mutations in the L1Cam gene. Hum. Mutat. 18: 1-12

Whitehorn D, Kopala LC (2002) Neuromotor dysfunction in Early Psychosis. An Clin Psychiatry 14: 113-121

Wilson GN, Pooley J, Rarker J (1982) The phenotype of ring chromosome 3. J Med Genet 19: 471-473

Wolf HK, Buslei R, Schmidt-Kastner R, Schmidt-Kastner PK, Pietsch T, Wiestler OD, Bluhmke I (1996) NeuN: a useful neuronal marker for diagnostic histopathology. J Histochem Cytochem 44: 1167-1171

Wood GK, Tomasiewicz H, Rutishauser U, Magnuson T, Quirion R, Rochford J, Srivastava LK (1998) NCAM-180 knockout mice display increased lateral ventricle size and reduced prepulse inhibition of startle. Neuroreport 9: 461-466

Wright P, Gill M, Murray RM (1993) Schizophrenia: genetics and the maternal immune response to viral infection. Am J Med Genet 48: 40-46

Zhang Y, Roslan R, Lang D, Schachner M, Lieberman AR, Anderson PN (2000) Expression of CHL1 and L1 by neurons and glia following sciatic nerve and dorsal root injury. Mol Cell Neurosci 16: 71-86

8 ABBREVIATIONS

Ab	Antibodies
C	Cingulate cortex
CA	Cornu ammon
$CaCl_2$	Calcium chloride
CALL	Cell adhesion L1 like
CAM	Cell Adhesion Molecule
CAT	Computer assisted tomography
cDNA	Complementary desoxyribonucleic acid
Cg1, Cg2	Cingulum 1, Cingulum 2
CHL1	Close homologue of L1
CHL1-/-	CHL1 deficient
CHL1+/+	CHL1 non deficient
cm	centimetres
cm^2	Square centimetres
cm^3	Cubic centimetres
CNPase	2´,3´-Cyclic Nucleotide 3´-Phosphodiesterase
CNS	Central nervous system
CRASH	Corpus callosum hypoplasia, retardation, adducted thumbs, spastic paraplegia and hydrocephalus
CSF	Cerebro spinal fluid
CST	Cortico spinal tract
CT	Computed tomography
Cy3	indocarbocyanin, red fluorescence dye
D2 receptor	Dopamine 2 receptor
DA	Dopamine
DSM IV	Diagnostic and statistical manual of mental disorders
ECM	Extracellular matrix
e.g.	example given
EPSS	Extrapyramidal signs and symptoms
est.	estimated
FN	Fibronectin
g	gramm
GABA	Gamma amino butyric acid
GAD	Glutamate decarboxylase
GAT1	GABA transporter 1
gt	genotype
HR studies	High risk studies
ICD10	International classification of diseases 10
i.e.	id est (that is)
Ig	Immunoglobulin
ip	intraperitoneal
IQ	Intelligence quotient
kD	kilodalton
ko	knockout
l	litre
LTP	Long term potentiation
M	Motor cortex
M	molar

m	metre
mm	milimetre (Metre $\times 10^{-3}$)
ml	mililitre (Litre $\times 10^{-3}$)
mo	months
MRI	Magnetic resonance imaging
mRNA	messenger ribonucleic acid
M1-M2	Motor cortex 1, Motor cortex 2
NaOH	Sodium hydroxide solution
NaN$_3$	Sodium azide
NCAM	Neural cell adhesion molecule
NCAM-/-	NCAM deficient
NCAM+/+	NCAM non deficient
NGS	Normal goat serum
NeuN	Neuron specific nuclear antigen
NgCAM	Neuron-glial Cell Adhesion Molecule
NGS	Normal Goat Serum
nm	nanometres
NrCAM	NgCAM related Cell Adhesion Molecule
PBS	Phosphate Buffered Saline
PCR	Polymerase Chain Reaction
PFC	PreFrontal Cortex
pH	p(otential) of H(ydrogen), the logarithm of the reciprocal of hydrogen-ion concentration in gram atoms per litre
PNS	Peripheral nervous system
PPI	Prepulse inhibition
PSA	Poly sialic acid
PV	Parvalbumin
RT	Room temperature
S	Sensory cortex
SD	Standard deviation
SPF	Specific pathogen-free
TH	Tyrosine hydroxylase
T	Section thickness
V	Volume
VH	Ventral hippocampus
VTA	Ventral tegmental area
v/v	volume per volume
wt	wildtype
w/v	weight per volume
ZMNH	Zentrum für Molekulare Neurobiologie Hamburg
%	Percent
3D	Three dimensional
μ	Micro (10^{-6})
°C	Grad Celsius

9 ACKNOWLEDGEMENT/DANKSAGUNG

10 CURRICULUM VITAE

<u>Personal Data</u>

Family Name	Thilo
First Name	Barbara Elisabeth
Date of Birth	18.04.1978
Place of Birth	Bonn, Germany
Nationality	German
Confession	Roman Catholic

<u>Education</u>

1984-1988	Paul-Gerhardt-Grundschule, Bonn, Germany
1988-1997	Kardinal-Frings-Gymnasium, Bonn, Germany
1995	Clayesmore School, Dorset, Great Britain
Sept. 1997 Feb. 1998	"Au-pair" position in Cleveland, OH, U.S.A
1998-2001	Regular student of medicine, Rheinische Friedrich-Wilhelms-Universität, Bonn, Germany
2001-2002	Regular student of medicine Universidad de Valencia, Spain
2002-2003	Doctoral candidate under supervision of Prof. Dr. Melitta Schachner, Zentrum für Molekulare Neurobiologie, Hamburg. Fellow of the "Deutsche Forschungsgemeinschaft" (German Research Foundation)
since 2003	Regular student of medicine Universität Hamburg, Germany
Oct. 2004- Feb.2005	Massachusetts General Hospital, Department of Neurology, Harvard Medical School, Boston, MA, USA

11 EIDESSTATTLICHE VERSICHERUNG

Ich versichere ausdrücklich, dass ich die Arbeit selbständig und ohne fremde Hilfe verfasst, andere als die von mir angegebenen Quellen und Hilfsmittel nicht benutzt und die aus den benutzten Werken wörtlich oder inhaltlich entnommenen Stellen einzeln nach Ausgabe (Auflage und Jahr des Erscheinens), Band und Seite des benutzten Werkes kenntlich gemacht habe.

Ferner versichere ich, dass ich die Dissertation bisher nicht einem Fachvertreter an einer anderen Hochschule zur Überprüfung vorgelegt oder mich anderweitig um Zulassung zur Promotion beworben habe.

_____

Barbara Elisabeth Thilo